Chapter VI
Extended Natural Neighbours Method

Content

Summary

In chapter V, the natural neighbours method was extended to the domain of 2D linear elastic fracture mechanics (LEFM) based on the FRAEIJS de VEUBEKE variational principle which allows assumptions on the displacement field, the stresse field, the strain field and the surface distributed support reactions field.

The basic idea is to take advantage of the flexibility of the FdV variational principle and to introduce, near the crack tips, stress and strain assumptions inspired from the analytical solution provided by the LEFM [WESTERGAARD, H.M. (1939)].

This has been done by introducing a node at each crack tip and by introducing these stress and strain assumptions in the corresponding Voronoi cell. In this approach, the crack lip has to be conformed to the edges of the Voronoi cell.

The present chapter develops an eXtended Natural nEighbours Method (XNEM) to solve 2D problems of LEFM.

In the proposed method, the crack is represented by a line that does not conform to the nodes or to the edges of the Voronoi cells.

The 2D domain contains N nodes (including nodes on the domain contour) but there is no node at the crack tips. The N Voronoi cells corresponding these nodes are built.

Then the discretization of the displacement field is enriched with Heaviside functions but not with crack tip functions since the experience of chapter V (section V.7) has shown that such an enrichment does not significantly improve the solution.

We have 3 types of cells:

- cells of type *O* that do not contain a crack;
- cells of type *H* that are divided into 2 parts by a crack;
- cells of type *C* that contain a crack tip.

We admit the discretization hypotheses separately in the 3 different types of cells.

For ordinary cells:

1. The assumed stresses are constant over an ordinary cell *I*.
2. The assumed strains are constant over an ordinary cell *I*.
3. The assumed support reactions are constant over each edge of ordinary Voronoi cells on which displacements are imposed.

For cells of type H that are cut into 2 parts by a crack:

1. The assumed stresses are constant over each part of the cell.
2. The assumed strains are constant over each part of the cell.
3. The assumed support reactions are piecewise constant over the edges on which displacements are imposed

For cells of type C that contain a crack tip, the stress and strain fields are enriched in a similar way as the LFMVCs of chapter V, i.e. by introducing in the stress and strain discretizations the solutions of the LEFM [WESTERGAARD, H.M. (1939)] for mode 1 and mode 2.

Introducing all the assumptions and enrichments in the FdV variational principle produces the set of equations governing the discretized solid.

As same as in the method developed in chapter V, the stress intensity coefficients are obtained as primary variables of the solution in the present method.

These equations are recast in matrix form and it is shown that the discretization parameters associated with the assumptions on the stresses and on the strains can be eliminated at the Voronoi cell level so that the final system of equations only involves the nodal displacements, the assumed support reactions and the stress intensity coefficients.

These support reactions can be further eliminated from the equation system if the imposed support conditions only involve displacements imposed as constant (in particular displacements imposed to zero) on a part of the solid contour.

The following properties, already obtained for the method of chapter V, remain valid:

In the cells of types O and H:

1. In the absence of body forces, the calculation of integrals over the area of the domain is avoided: only integrations on the edges of the Voronoi cells are required.
2. The derivatives of the Laplace interpolation functions are not required.

In the cells of type C:

1. Some integrations on the area of these cells are required but they can be calculated analytically.
2. The other integrals are integrals on the edges of these cells
3. The derivatives of the Laplace interpolation functions are not required

Applications to the mode 1 test, mode 2 test and single edge crack test are performed. The results validate this method and nearly incompressibility locking is avoided.

VI.1. Introduction

In chapter V, a new approach to solve problems of Linear Elastic Fracture Mechanics (LEFM) has been developed.

The basic idea was to take advantage of the flexibility of the FdV variational principle and to introduce, near the crack tips, stress and strain assumptions inspired from the analytical solution provided by the Theory of Elasticity [WESTERGAARD, H.M. (1939)].

This has been done by imposing a node at each crack tip and by introducing these stress and strain assumptions in the corresponding Voronoi cell called Linear Fracture Mechanics Voronoi Cell (LFMVC).

In the present chapter, a different approach is proposed in which it is not necessary to locate nodes at the crack tips.

It is somehow inspired from the eXtended Finite Element Method (XFEM) that was initially developed by [MOES N. et al. (1999), DOLBOW J.E. (1999)] for a single crack in 2D problems.

The XFEM is an approach based on the virtual work principle and, consequently, the primary unknowns are the displacements.

The fundamental idea is to define the crack by a line that does not conform to the finite element edges (figure VI.1) and to enrich the discretization of the displacement field.

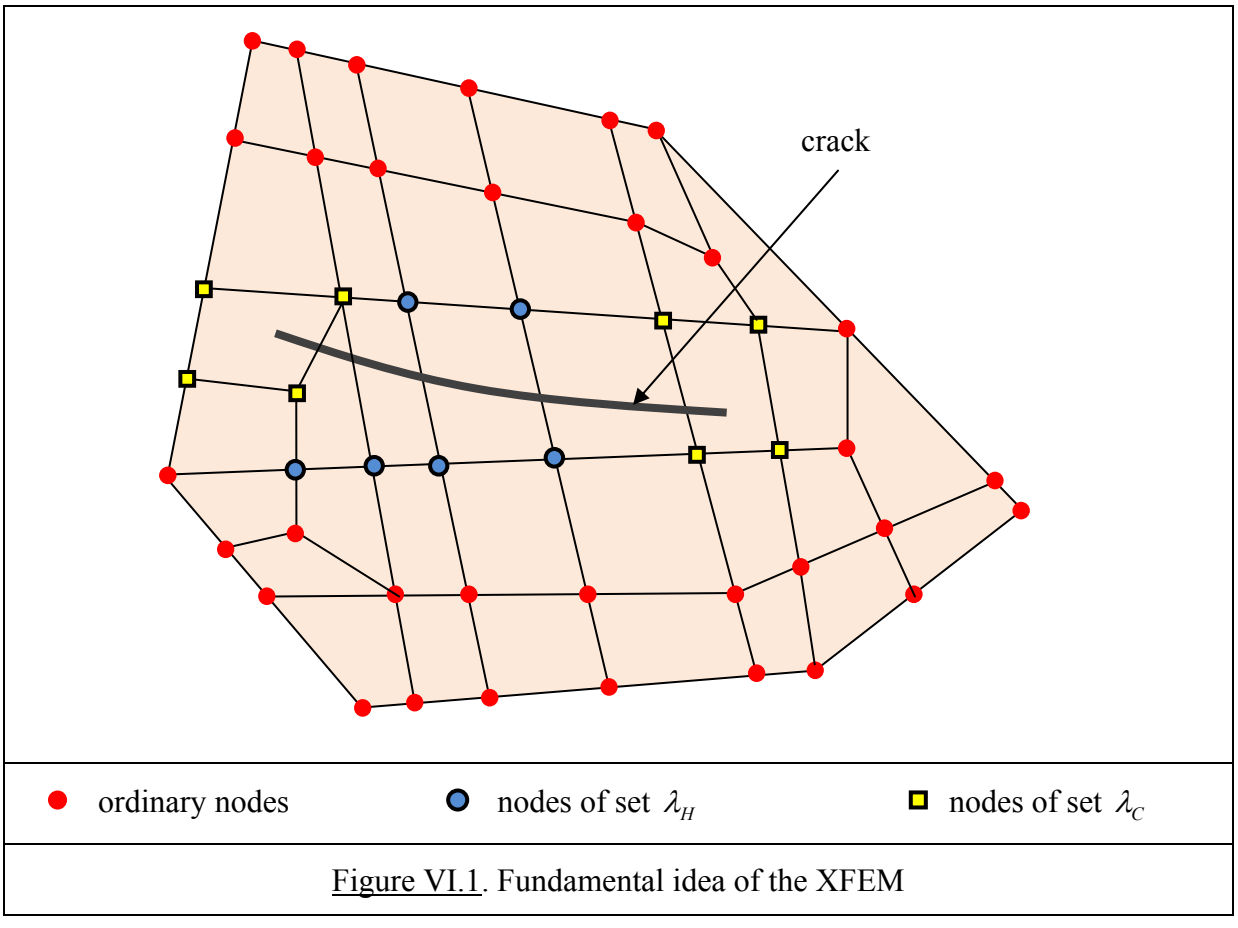

Figure VI.1. Fundamental idea of the XFEM

Let λ_H be the set of nodes the shape function support of which is cut by the crack.

Let λ_C be the set of nodes shape function support of which contains the crack tips.

The displacement field is discretized by:

$$u_i = \sum_{J=1}^{N} \Phi_J \, u_i^J + \sum_{J \in \lambda_H} H(\underline{X}) \, \Phi_J \, b_i^J + \sum_{J \in \lambda_C} \Phi_J \left[\sum_{k=1}^{4} c_k^J \, F_k(\underline{X}) \right] \tag{VI.1}$$

where

Φ_J is the usual finite element shape function associated with node J;

$H(\underline{X})$ is a Heaviside function : $H(\underline{X}) = \begin{cases} +1 & \text{on one side of the crack} \\ -1 & \text{on the other side of the crack} \end{cases}$ (VI.2)

$F_k(\underline{X})$ is a set of 4 functions inspired by the displacement field near a crack tip for mode 1 and mode 2:

$$F_1(r,\theta) = \sqrt{r} \, \sin\frac{\theta}{2} \tag{VI.3.a}$$

$$F_2(r,\theta) = \sqrt{r} \, \cos\frac{\theta}{2} \tag{VI.3.b}$$

$$F_3(r,\theta) = \sqrt{r} \, \sin\frac{\theta}{2} \, \cos\theta \tag{VI.3.c}$$

$$F_4(r,\theta) = \sqrt{r} \, \cos\frac{\theta}{2} \, \sin\theta \tag{VI.3.d}$$

with (r,θ) the polar coordinates at the crack tip (see chapter II, section II.4.5).

In addition to the usual degrees of freedom u_i^J (the nodal displacements),

- the b_i^J are new displacement parameters taking account of the displacement discontinuity through the crack;
- the c_k^J are new displacement parameters taking account of the particular form of the displacement field near the crack tips.

This type of enrichment is called a “topological enrichment”.

This elegant approach simplifies the meshing operations since it is not necessary to make the crack lips coincide with element edges and, consequently, is well suited for the modelling of crack propagation without remeshing.

Furthermore, it takes account of the particular form of the displacements near the crack tips which improves the quality of the results.

The method has been extended to 3D cases [SUKUMAR N. et al. (2000)], to the modelling of cracks in plates [DOLBOW J. et al. (2000-a) and (2000-b)], to the case of branched and intersecting cracks [DAUX C. et al. (2000)], to the case of higher order elements [STAZI F.L. et al. (2003)], to the case of bimaterials interfaces [SUKUMAR N. et al. (2004)], …

In [STOLARSKA M. et al. (2001)], it has been coupled with the “level set method” [OSHER S.A. (1999)] for representing and propagating the crack.

It has also been proposed [BECHET E. et al. (2005)] to replace the "topological" enrichment, in which only the elements touching the crack are enriched, by a "geometrical" enrichment in which a given domain size is enriched. This improved the quality of the results.

It is also worth mentioning that in [DOLBOW J. and DEVAN A. (2004)], an assumed strain enrichment is proposed in which the 2 parts of the finite elements cut by the crack are separately enriched by an assumed strain field. The development of the method relies on the HU-WASHIZU variational principle (chapter II, section II.3.1). In this paper, the enrichment of the displacement filed is limited to the first 2 terms of (VI.1), which means that the enrichment of the nodes of the set λ_C is not included.

The present chapter develops an eXtended Natural nEighbours Method (XNEM) to solve 2D problems of LEFM.

In the proposed method, the crack is also represented by a line that does not conform to the nodes or to the edges of the Voronoi cells.

Then the discretization of the displacement field is enriched with Heaviside functions as (VI.2) but not with crack tip functions of the type (VI.3) since the experience of chapter V shows that such an enrichment does not significantly improve the solution (see section V.7).

On the other hand, the stress and strain assumptions in the cells cut by the crack are enriched by considering, in each of the two parts, different constant stresses and constant strains.

Finally, for the cells containing the crack tips, the stress and strain fields are enriched in a similar way as the LFMVC cells of chapter V, i.e. by introducing in the stress and strain discretizations the solutions of the Theory of Elasticity [WESTERGAARD, H.M. (1939)] for mode 1 and mode 2.

Since the purpose is to explore a new numerical method, the options retained for the development are the simplest ones:

- there is a single crack with 1 or 2 tips;
- it does not propagate;
- the "topological" enrichment rather than the "geometrical" enrichment is chosen

These limitations could obviously be eliminated taking advantage of the existing techniques used for the XFEM, but this is outside the scope of the present thesis.

VI.2. Domain decomposition

In the natural neighbours method, the domain contains N nodes (including nodes on the domain contour) and the N Voronoi cells corresponding to these nodes are built.

The area of the domain is:

$$A = \sum_{I=1}^{N} A_I \tag{VI.4}$$

with A_I the area of Voronoi cell I.

If cracks are present in the domain, we have 3 types of cells:

- cells of type O (figure VI.3) that do not contain a crack;
- cells of type H (figure VI.4) that are divided into 2 parts by a crack;
- cells of type C (figure VI.5) that contain a crack tip.

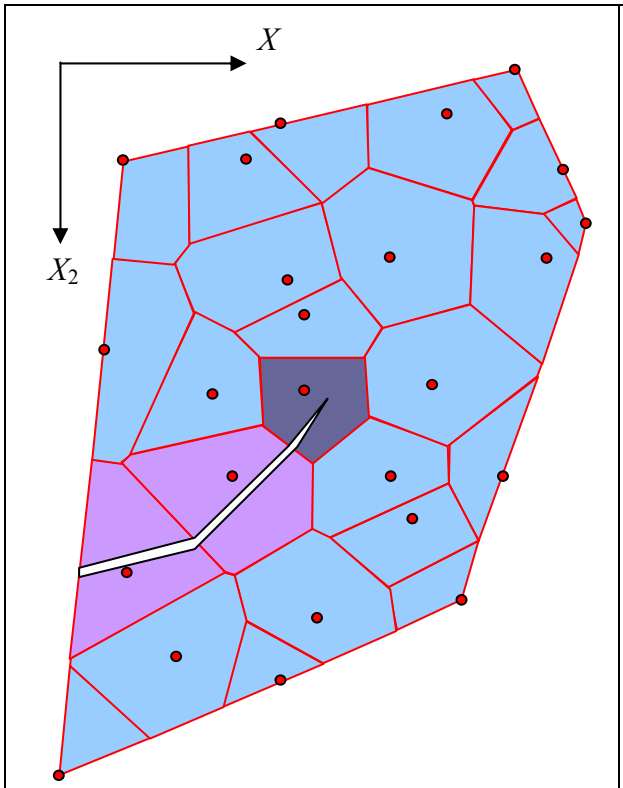

Figure VI.2. Domain decomposition

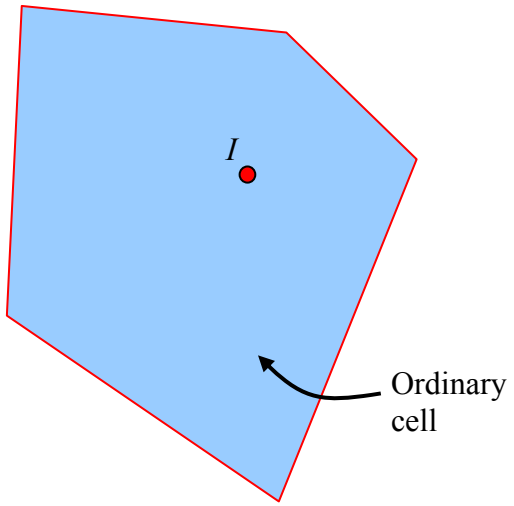

Figure VI.3. Cell of type O

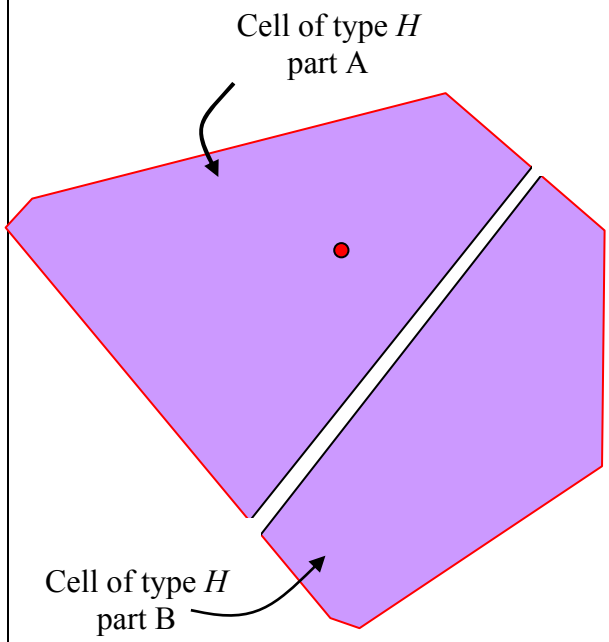

Figure VI.4. Cell of type H

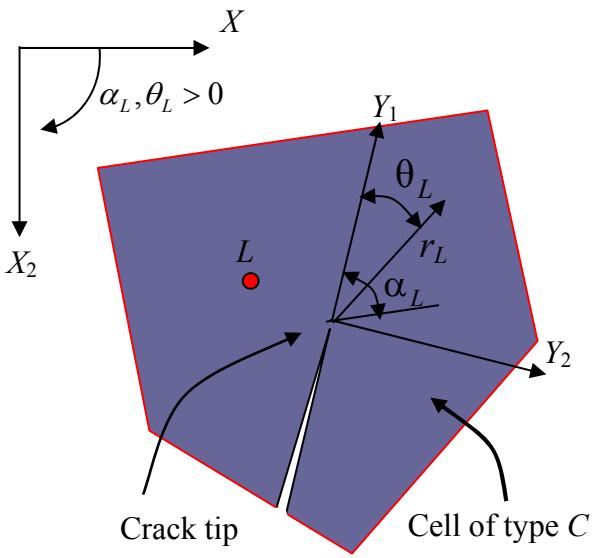

Figure VI.5. Cell of type C

Note that there may be several cells of type *C* if there are several cracks or even a single crack the 2 tips of which are inside the domain.

We could also have a cell containing several crack tips (type *C*+*C*) or a cell divided into several parts by several cracks (type *H*+*H*) or a cell divided in 2 parts by a crack and containing a crack tip (type *H*+*C*).

Here, we only consider cells of types *O*, *H* and *C*.

In addition, for simplicity, we consider that there is only 1 crack and that, in each cell, the crack is straight.

Let N_O, N_H, N_C be the numbers of cells of types *O*, *H* and *C* respectively with

$$N = N_O + N_H + N_C \tag{VI.5}$$

the total number of cells.

VI.3. Discretization

VI.3.1. Discretization of $\varepsilon_{ij}, \Sigma_{ij}, r_i$ in cells of type *O*

We admit the following discretization hypotheses for ordinary cells:

1. The assumed stresses Σ_{ij} are constant over an ordinary cell *I*:

$$\Sigma_{ij} = \Sigma_{ij}^I \qquad I = 1, N_O \tag{VI.6}$$

2. The assumed strains ε_{ij} are constant over an ordinary cell *I*:

$$\varepsilon_{ij} = \varepsilon_{ij}^I \qquad I = 1, N_O \tag{VI.7}$$

3. The assumed support reactions t_i are constant over each edge *K* of ordinary Voronoi cells on which displacements are imposed

$$r_i = r_i^K \tag{VI.8}$$

VI.3.2. Discretization of $\varepsilon_{ij}, \Sigma_{ij}, r_i$ in cells of type *H*

As shown on figure VI.4, the cell is divided into 2 parts *A* and *B* by the crack.

We admit the following discretization hypotheses for cells of type *H*:

1. The assumed stresses Σ_{ij} are constant over each part of the cell:

$$\Sigma_{ij} = \Sigma_{ij}^{A,I} \text{ in part } A \text{ of cell } I \qquad I = 1, N_H \tag{VI.9-a}$$

$$\Sigma_{ij} = \Sigma_{ij}^{B,I} \text{ in part } B \text{ of cell } I \qquad I = 1, N_H \tag{VI.9-b}$$

2. The assumed strains ε_{ij} are constant over each part of the cell:

$$\varepsilon_{ij} = \varepsilon_{ij}^{A,I} \text{ in part } A \text{ of cell } I \qquad I = 1, N_H \tag{VI.10-a}$$

$\varepsilon_{ij} = \varepsilon_{ij}^{B,I}$ in part B of cell I $\quad I = 1, N_H$ (VI.10-b)

3. The assumed support reactions r_i are piecewise constant over the edges K on which displacements are imposed

$r_i = r_i^K$ on the whole edge K if it is not cut by the crack (VI.11-a)

$r_i = r_i^{A,K}$ on part A of edge K if it is cut by the crack (VI.11-b)

$r_i = r_i^{B,K}$ on part B of edge K if it is cut by the crack (VI.11-c)

VI.3.3. Discretization of $\varepsilon_{ij}, \Sigma_{ij}, r_i$ in cells of type *C*

It was recalled in Chapter II, section II.4.5. that, in LEFM, the stress fields near the crack tip (figure VI.5) are given by:

for mode 1:
$$\begin{Bmatrix} \tau_{11} \\ \tau_{22} \\ \tau_{12} \end{Bmatrix} = \frac{K_1}{\sqrt{2\pi r_L}} cos\frac{\theta_L}{2} \begin{Bmatrix} 1 - sin\frac{\theta_L}{2} \; sin\frac{3\theta_L}{2} \\ 1 + sin\frac{\theta_L}{2} \; sin\frac{3\theta_L}{2} \\ -sin\frac{\theta_L}{2} \; cos\frac{3\theta_L}{2} \end{Bmatrix} \quad \text{(VI.12)}$$

for mode 2:
$$\begin{Bmatrix} \tau_{11} \\ \tau_{22} \\ \tau_{12} \end{Bmatrix} = \frac{K_2}{\sqrt{2\pi r_L}} \begin{Bmatrix} -sin\frac{\theta_L}{2}(2 + cos\frac{\theta_L}{2} \; cos\frac{3\theta_L}{2}) \\ cos\frac{\theta_L}{2} sin\frac{\theta_L}{2} \; cos\frac{3\theta_L}{2} \\ cos\frac{\theta_L}{2}(1 - sin\frac{\theta_L}{2} \; sin\frac{3\theta_L}{2}) \end{Bmatrix} \quad \text{(VI.13)}$$

These stresses are expressed in the local frame (Y_1, Y_2) attached to the crack tip (figure VI.5).

K_1 and K_2 are the stress intensity factors of modes 1 and 2 respectively.

These stresses are valid for both plane stress and plane strain conditions.

In order to have a better representation of the stresses in the vicinity of the crack tip, we admit the following discretization hypotheses for cells of type *C*:

1. The assumed stresses are given in the local frame $(Y_1, Y_2)_L$ attached to the crack tip by:

$$\begin{Bmatrix} P_{11} \\ P_{22} \\ P_{12} \end{Bmatrix}^L = \begin{Bmatrix} P_{11}^O \\ P_{22}^O \\ P_{12}^O \end{Bmatrix}^L + \begin{Bmatrix} P_{11}^\Sigma \\ P_{22}^\Sigma \\ P_{12}^\Sigma \end{Bmatrix}^L \Leftrightarrow \{P\}^L = \{P^O\}^L + \{P^\Sigma\}^L, \; L = 1, N_C \quad \text{(VI.14)}$$

with

$$\{P^\Sigma\}^L = f(r_L)\left[K_{\Sigma 1}^L \{g_1(\theta_L)\} + K_{\Sigma 2}^L \{g_2(\theta_L)\}^L\right] = K_{\Sigma 1}^L \{H_1\}^L + K_{\Sigma 2}^L \{H_2\}^L \quad \text{(VI.15)}$$

$$\{g_1(\theta)\}=\cos\frac{\theta}{2}\begin{Bmatrix}1-\sin\frac{\theta}{2}\ \sin\frac{3\theta}{2}\\ 1+\sin\frac{\theta}{2}\ \sin\frac{3\theta}{2}\\ -\sin\frac{\theta}{2}\ \cos\frac{3\theta}{2}\end{Bmatrix};\quad \{g_2(\theta)\}=\begin{Bmatrix}\sin\frac{\theta}{2}(2+\cos\frac{\theta}{2}\ \cos\frac{3\theta}{2})\\ -\cos\frac{\theta}{2}\sin\frac{\theta}{2}\ \cos\frac{3\theta}{2}\\ \cos\frac{\theta}{2}(1-\sin\frac{\theta}{2}\ \sin\frac{3\theta}{2})\end{Bmatrix};$$

$$f(r)=\frac{1}{\sqrt{2\pi r}} \qquad \text{(VI.16)}$$

$$\{H_1\}^L=f(r_L)\{g_1(\theta_L)\};\quad \{H_2\}^L=f(r_L)\{g_2(\theta_L)\} \qquad \text{(VI.17)}$$

$K_{\Sigma 1}^L$ and $K_{\Sigma 2}^L$, L=1,N_C are stress parameters associated with the cells of type C.

Of course, the stresses Σ_{ij}^L in the global frame (X_1, X_2) can be obtained by tensor rotation.

2. The assumed strains are interpolated by:

$$\begin{Bmatrix}\gamma_{11}\\ \gamma_{22}\\ 2\gamma_{12}\end{Bmatrix}^L=\begin{Bmatrix}\gamma_{11}^O\\ \gamma_{22}^O\\ 2\gamma_{12}^O\end{Bmatrix}^L+\begin{Bmatrix}\gamma_{11}^\Sigma\\ \gamma_{22}^\Sigma\\ 2\gamma_{12}^\Sigma\end{Bmatrix}^L \quad\Leftrightarrow\quad \{\gamma\}^L=\{\gamma^O\}^L+\{\gamma^\varepsilon\}^L \qquad \text{(VI.18-a)}$$

$$\{\gamma^\Sigma\}^L=[D]^L\{K_{\Sigma 1}^L\{H_1\}^L+K_{\Sigma 2}^L\{H_2\}\} \qquad \text{(VI.18-b)}$$

with

$$[D]^L=\frac{1}{E_L^*}\begin{bmatrix}1 & -\nu_L^* & 0\\ -\nu_L^* & 1 & 0\\ 0 & 0 & 2(1+\nu_L^*)\end{bmatrix} \qquad \text{(VI.19)}$$

$$E_L^*=\begin{cases}\dfrac{E_L}{1-\nu_L^2} & \text{in plane strain state}\\ E_L & \text{in plane stress state}\end{cases}\qquad \nu_L^*=\begin{cases}\dfrac{\nu_L}{1-\nu_L} & \text{in plane strain state}\\ \nu_L & \text{in plane stress state}\end{cases} \qquad \text{(VI.20)}$$

These strains are also given in the local frame $(Y_1,Y_2)_L$ attached to the crack tip and can be rotated into the global frame if necessary.

The elastic parameters E_L, ν_L can be different in different cells if necessary.

$K_{\Sigma 1}^L$ and $K_{\Sigma 2}^L$ constitute an additional set of displacement discretization parameters associated with the cells of type C.

3. The assumed support reactions r_i are piecewise constant over the edges K on which displacements are imposed:

$r_i=r_i^K$ on the whole edge K if it is not cut by the crack (VI.21-a)

$r_i = r_i^{A,K}$ on part A of edge K if it is cut by the crack (VI.21-b)

$r_i = r_i^{B,K}$ on part B of edge K if it is cut by the crack (VI.21-c)

The situation corresponding to (VI.21-b) and (VI.21-c) is illustrated on figure VI.6.

On parts A and B of the edge cut by the crack, it is possible to impose different displacements $\tilde{u}_i^A$ and $\tilde{u}_i^B$.

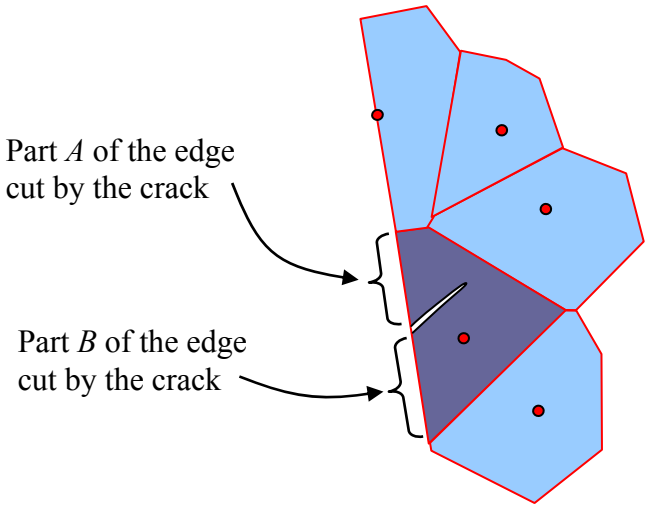

Figure VI.6. Crack cutting the domain contour

VI.3.4. Discretization of the displacements

Let us define the following sets.

- λ^H : the set of nodes corresponding to all the cells of type H (i.e. cut by the crack). This set has N_H elements.
- λ^C : the set of nodes corresponding to all the cells of type C (containing a crack tip). This set has N_C elements. In the present case, since we consider a single crack, N_C =1 or 2.
- Λ : the union of the sets λ^H and of the sets λ^C. Λ is the labelled as the set of crack nodes.

$$\Lambda = \lambda^H \cup \lambda^C$$

The discretization of the displacements is composed of two contributions

$$u_i = \sum_{J=1}^{N} \Phi_J u_i^J + \sum_{J \in \Lambda} C(\underline{X})\, \Phi_J\, a_i^J \qquad \text{(VI.22)}$$

where:

- u_i^J is the displacement of node J (corresponding to Voronoi cell J)
- Φ_J is the corresponding Laplace interpolant
- $C(\underline{X})$ is a function, labelled as the crack function, that will be defined precisely in section VI.3.5

- a_i^J is an additional set of displacement discretization parameters attached to the nodes belonging to the set Λ (the set of crack nodes)

The first term is the usual interpolation of the natural neighbours method.

The second term will be designed to allow a displacement discontinuity through the crack.

VI.3.5. Definition of the crack function *C(X)*

The idea is to make *C(X)* equal to +1 on one side of the crack and to -1 on the other side.

However, care must be taken for its definition ahead of the crack tips where it can take different values.

Let $C_1 - C_1^*$ and $C_2 - C_2^*$ be 2 straight lines having the same directions as the 2 crack ends (figure VI.7). They define 2 sub-domains A_A and A_B in which a function $H(\underline{X})$ is given by:

$H(\underline{X}) = +1 \quad if \quad \underline{X} \in A_A$

$H(\underline{X}) = -1 \quad if \quad \underline{X} \in A_B$

Let $A_1 - B_1$ and $A_2 - B_2$ be 2 straight lines perpendicular to the 2 crack ends (figure VI.8).

Let $A_1^* - B_1^*$ and $A_2^* - B_2^*$ be 2 straight lines parallel to $A_1 - B_1$ and $A_2 - B_2$ respectively. They are such that their points P_1 and P_2 are located on the crack at a user defined distance from the corresponding crack tips (figure VI.8). It is assumed that the crack is straight on $C_1 - P_1$ as well as on $C_2 - P_2$.

In the example of figure VI.8, points P_1 and P_2 are located at the intersection of the crack with the edge of the cell of type C.

Figure VI.9 shows a zoom on crack tip 1. The subscript 1 is omitted for simplicity.

Line $A - B$ is oriented by the abcissa s such that $s = 0$ at point C and $s > 0$ as indicated on the figure (at 90° counterclockwise with respect to the direction of the crack tip).

Any point X inside the domain belongs to a line $C - X - Q$ intersecting $A^* - B^*$ at point Q. This line is oriented by the abcissa ξ such that $\xi = 0$ at point C and $\xi = 1$ at point Q.

Hence, point X can be referred to by the skew coordinates (s,ξ) attached to the crack tip. They can be deduced from its cartesian coordinates (X_1, X_2) by simple geometrical considerations developed in annex 4.

The same can also be done for crack tip 2.

So, any point (X_1, X_2) in the domain has skew coordinates (s_1, ξ_1) with respect to crack tip 1 and (s_2, ξ_2) with respect to crack tip 2.

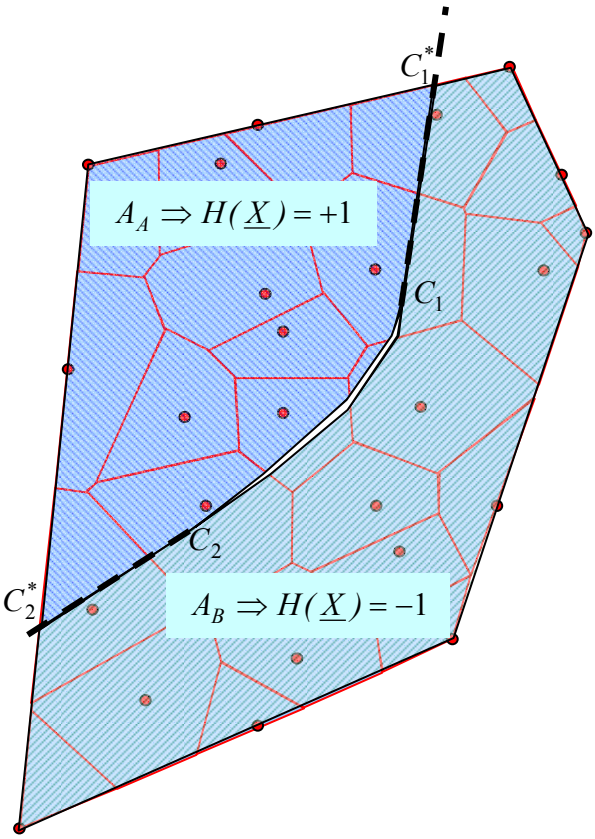

Figure VI.7. The two sides of a crack.

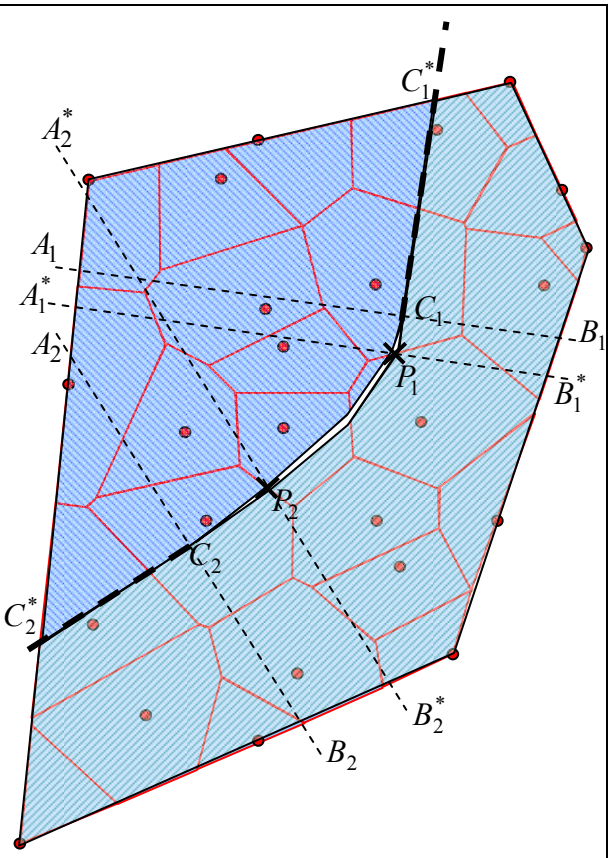

Figure VI.8. The different zones for $C(\underline{X})$.

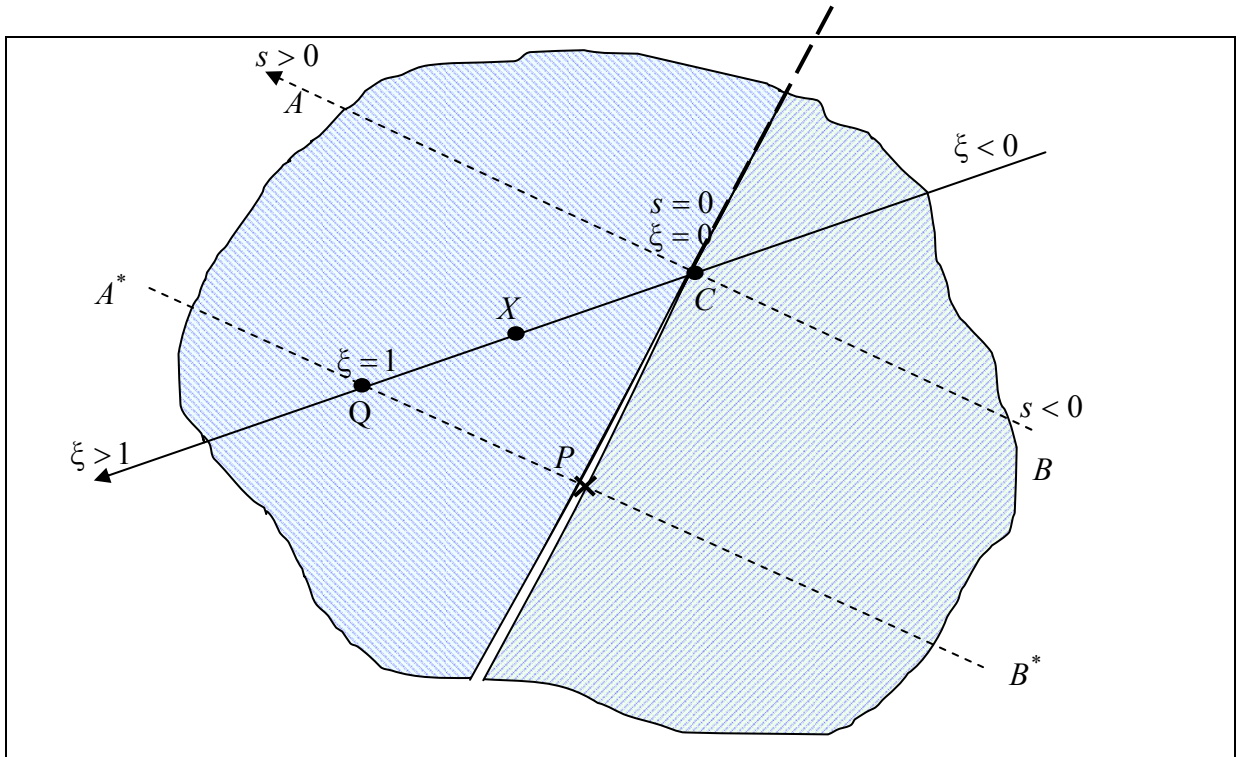

Figure VI.9. Zoom on a crack tip

With the help of these skew coordinates, the crack function $C(\underline{X})$ is defined as follows:

$$\begin{aligned}
&if \quad \xi_1 < 0 \; or \; \xi_2 < 0 && \Rightarrow \quad C = 0 \\
&if \quad \xi_1 \geq 1 \; and \; \xi_2 \geq 1 && \Rightarrow \quad C = H \\
&if \quad 0 < \xi_1 < 1 \; and \; \xi_2 \geq 1 && \Rightarrow \quad C = H\sqrt{\xi_1} \\
&if \quad 0 < \xi_2 < 1 \; and \; \xi_1 \geq 1 && \Rightarrow \quad C = H\sqrt{\xi_2} \\
&if \quad 0 < \xi_2 < 1 \; and \; 0 < \xi_1 < 1 && \Rightarrow \quad C = H\sqrt{\xi_1 \xi_2}
\end{aligned} \tag{VI.23}$$

Examples of the crack function are given in annex 4.

VI.4. Discretization of the FdV variational principle

We start from the FdV variational principle introduced in chapter II and we recall its expression for completeness (we keep the equation numbers of chapter II).

$$\delta\Pi = \int_A (\sigma_{ij} - \Sigma_{ij})\delta\varepsilon_{ij} dA - \int_A (\frac{\partial \Sigma_{ji}}{\partial X_j} + F_i)\delta u_i dA + \int_A \delta\Sigma_{ij}\left[\frac{1}{2}(\frac{\partial u_i}{\partial X_j} + \frac{\partial u_j}{\partial X_i}) - \varepsilon_{ij}\right] dA$$

$$+ \int_{S_u} (N_j \Sigma_{ji} - r_i)\delta u_i dS + \int_{S_t} (N_j \Sigma_{ji} - T_i)\delta u_i dS = 0 \tag{II.36}$$

or

$$\delta\Pi = \delta\Pi_1 + \delta\Pi_2 + \delta\Pi_3 + \delta\Pi_4 + \delta\Pi_5 + \delta\Pi_6 = 0 \tag{II.31}$$

with the different terms

$$\delta\Pi_1 = \int_A \delta W(\varepsilon_{ij}) dA = \int_A \sigma_{ij}\delta\varepsilon_{ij} dA \tag{II.25}$$

$$\delta\Pi_2 = \int_A \Sigma_{ij}\left[\frac{1}{2}(\frac{\partial \delta u_i}{\partial X_j} + \frac{\partial \delta u_j}{\partial X_i}) - \delta\varepsilon_{ij}\right] dA \tag{II.26}$$

$$\delta\Pi_3 = \int_A \delta\Sigma_{ij}\left[\frac{1}{2}(\frac{\partial u_i}{\partial X_j} + \frac{\partial u_j}{\partial X_i}) - \varepsilon_{ij}\right] dA \tag{II.27}$$

$$\delta\Pi_4 = -\int_A F_i \, \delta u_i \, dA \tag{II.28}$$

$$\delta\Pi_5 = -\int_{S_t} T_i \, \delta u_i \, dS \tag{II.29}$$

$$\delta\Pi_6 = \int_{S_u} \delta r_i (\tilde{u}_i - u_i) dS - \int_{S_u} r_i \, \delta u_i \, dS \tag{II.30}$$

For the linear elastic case, the stresses are given by:

$$\sigma_{ij} = \frac{\partial W(\varepsilon_{ij})}{\partial \varepsilon_{ij}} \tag{II.34}$$

and

$$W(\varepsilon_{ij}) = \frac{1}{2} C_{ijkl} \, \varepsilon_{ij} \, \varepsilon_{kl} \tag{II.35}$$

where C_{ijkl} is the classical Hooke's tensor.

In (II.29) and (II.30), the integrals are computed along the domain contour. This contour is the union of some of the edges of the exterior Voronoi cells. These edges are denoted by S_K and we have

$$S = \sum_{K=1}^{M} S_K \; ; \quad S_u = \sum_{K=1}^{M_u} S_K \; ; \quad S_t = \sum_{K=1}^{M_t} S_K \; ; \qquad S = S_u \cup S_t \Rightarrow M = M_u + M_t \tag{VI.24}$$

where M is the number of edges composing the contour, M_u the number of edges on which displacements $\tilde{u}_i$ are imposed and M_t the number of edges on which surface tractions T_i are imposed.

Using the domain decomposition, these terms become:

$$\delta\Pi_1 = \sum_{I=1}^{N} \int_{A_I} \left(\sigma_{ij} - \Sigma_{ij}\right) \delta\varepsilon_{ij} \, dA_I \tag{VI.25}$$

$$\delta\Pi_2 = \sum_{I=1}^{N} \int_{A_I} \Sigma_{ij} \left[\frac{1}{2} \left(\frac{\partial \delta u_i}{\partial X_j} + \frac{\partial \delta u_j}{\partial X_i} \right) \right] dA_I \tag{VI.26}$$

$$\delta\Pi_3 = \sum_{I=1}^{N} \int_{A_I} \delta\Sigma_{ij} \left[\frac{1}{2} \left(\frac{\partial u_i}{\partial X_j} + \frac{\partial u_j}{\partial X_i} \right) - \varepsilon_{ij} \right] dA_I \tag{VI.27}$$

$$\delta\Pi_4 = -\sum_{I=1}^{N} \int_{A_I} F_i \, \delta u_i \, dA_I \tag{VI.28}$$

$$\delta\Pi_5 = -\sum_{K=1}^{M_t} \int_{S_K} T_i \, \delta u_i \, dS_K \tag{VI.29}$$

$$\delta\Pi_6 = \sum_{K=1}^{M_u} \left[\int_{S_K} \delta r_i \left(\tilde{u}_i - u_i \right) dS_K - \int_{S_K} r_i \, \delta u_i \, dS_K \right] \tag{VI.30}$$

Introducing the discretizations of section VI.3 in the FdV variational principle (II.31) leads to the equations of table VI.1.

The details of the calculations are given in annex 5.

The next section is devoted to the solution of these equations and will be concluded by a complete summary of the variables and notations used in this chapter.

In particular, the different symbols and matrices appearing in table VI.1 are defined in tables VI.5 and VI.6.

In these equations only the matrices $[IH]^L$ and $[HDH]^L$ require an integration on the area of the cells of type C but these integrations can be performed analytically as in chapter V.

Table VI.1. Discretized equations for XNEM

Stress identification: the assumed stresses in cells of types *O*, *H* and *C* are equal to the constitutive stresses deduced from the assumed strains in those cells.	
$\{\Sigma\}^I = \{\sigma\}^I = [C]^I \{\varepsilon\}^I, \quad I = 1, N_O$	(VI.31-a)
$\{\Sigma\}^{A,J} = \{\sigma\}^{A,J} = [C]^J \{\varepsilon\}^{A,J}, \quad J \in \lambda_H$	(VI.31-b)
$\{\Sigma\}^{B,J} = \{\sigma\}^{B,J} = [C]^J \{\varepsilon\}^{B,J}, \quad J \in \lambda_H$	(VI.31-c)
$\{P^0\}^L = [C]^L \{\gamma^0\}^L, \quad L \in \lambda_C$	(VI.31-d)
$\{K_\Sigma\}^L = \{K_\Sigma\}^L, \quad L \in \lambda_C$	(VI.31-e)
Equilibrium equations associated with the degrees of freedom u_i^J of the cells of type *O*	
$\sum_{I=1}^{N_O} [A]^{IJ} \{\Sigma\}^I + \sum_{I \in \lambda_H} [A_A]^{IJ} \{\Sigma\}^{A,I} + \sum_{I \in \lambda_H} [A_B]^{IJ} \{\Sigma\}^{B,I} + \sum_{L \in \lambda_C} [R]^{L,T} \left[[W]^{JL} \{P^0\}^L + [V]^{JL} \{K_\Sigma\}^L \right]$ $= \sum_{I=1}^{N} \{\tilde{F}\}^{IJ} + \sum_{K=1}^{M_t} \{\tilde{T}\}^{IJ} + \sum_{K=1}^{M_u^O} B^{KJ} \{r\}^K + \sum_{K=1}^{M_u^A} B^{KJ} \{r\}^{A(K)} + \sum_{K=1}^{M_u^B} B^{KJ} \{r\}^{B(K)} \qquad J = 1, N$	(VI.32)
Equilibrium equations associated with the degrees of freedom a_i^J of the cells of type *H, C*	
$\sum_{I=1}^{N_O} [A_C]^{IJ} \{\Sigma\}^I + \sum_{I \in \lambda_H} [A_{C,A}]^{IJ} \{\Sigma\}^{A,I} + \sum_{I \in \lambda_H} [A_{C,B}]^{IJ} \{\Sigma\}^{B,I} + \sum_{L \in \lambda_C} [R]^{L,T} \left[[W_C]^{JL} \{P^0\}^L + [V_C]^{JL} \{K_\Sigma\}^L \right]$ $= \sum_{I=1}^{N} \{\tilde{F}_C\}^{IJ} + \sum_{K=1}^{M_t} \{\tilde{T}_C\}^{KJ} + \sum_{K=1}^{M_u^O} B_C^{KJ} \{r\}^K + \sum_{K=1}^{M_u^A} B_C^{KJ} \{r\}^{A(K)} + \sum_{K=1}^{M_u^B} B_C^{KJ} \{r\}^{B(K)} \quad , \quad J \in \Lambda$	(VI.33)
Compatibility equations in the cells of type *O*	
$A_I \{\varepsilon\}^I = \sum_{J=1}^{N} [A]^{IJ,T} \{u\}^J + \sum_{J \in \Lambda} [A_C]^{IJ,T} \{a\}^J, \quad I = 1, N_O$	(VI.34-a)
Compatibility equations in the cells of type *H*.	
$A_{A,I} \{\varepsilon\}^{A,I} = \sum_{J=1}^{N} [A_A]^{IJ,T} \{u\}^J + \sum_{J \in \Lambda} [A_{C,A}]^{IJ,T} \{a\}^J, \quad I \in \lambda_H$	(VI.34-b)
$A_{B,I} \{\varepsilon\}^{B,I} = \sum_{J=1}^{N} [A_B]^{IJ,T} \{u\}^J + \sum_{J \in \Lambda} [A_{C,B}]^{IJ,T} \{a\}^J, \quad I \in \lambda_H$	(VI.34-c)
Compatibility equations in the cells of type *C*.	
$A_L \{\gamma^0\}^L + [D]^L [IH]^L \{K_\Sigma\}^L = \sum_{I=1}^{N} [W]^{IL,T} \{v\}^{I,L} + \sum_{I \in \Lambda} [W_C]^{IL,T} \{b\}^{I,L}, \quad L \in \lambda_C$	(VI.34-d)
$[IH]^{L,T} \{\gamma^0\}^L + [HDH]^L \{K_\Sigma\}^L = \sum_{I=1}^{N} [V]^{IL,T} \{v\}^{I,L} + \sum_{I \in \Lambda} [V_C]^{IL,T} \{b\}^{I,L}, L \in \lambda_C$	(VI.34-e)

Compatibility equations with the imposed displacements on the boundaries on the edges of cells of type *O*.	
$\sum_{J=1}^{N} B^{KJ}\{u\}^J + \sum_{J\in\Lambda}^{N} B_C^{KJ}\{a\}^J = \{\widetilde{U}\}^K, \quad K=1,M_u^O$	(VI.35-a)
Compatibility equations with the imposed displacements on the boundaries on the edges of cells of type *H*.	
$\sum_{J=1}^{N} B^{KJ}\{u\}^J + \sum_{J\in\Lambda}^{N} B_C^{KJ}\{a\}^J = \{\widetilde{U}\}^{A(K)}, \quad K=1,M_u^A$	(VI.35-b)
$\sum_{J=1}^{N} B^{KJ}\{u\}^J + \sum_{J\in\Lambda}^{N} B_C^{KJ}\{a\}^J = \{\widetilde{U}\}^{B(K)}, \quad K=1,M_u^B$	(VI.35-c)

VI.5. Solution of the equations

VI.5.1. Stresses in terms of the displacement discretization parameters

Introducing (VI.34-a,b,c) in (VI.31-a,b,c), we get:

$$\{\Sigma\}^I = \left[C^*\right]^I \left[\sum_{J=1}^{N} [A]^{IJ,T}\{u\}^J + \sum_{J\in\Lambda}[A_C]^{IJ,T}\{a\}^J\right], \quad I=1,N_O \tag{VI.36-a}$$

$$\{\Sigma\}^{A,I} = \left[C^*\right]^I \left[\sum_{J=1}^{N} [A_A]^{IJ,T}\{u\}^J + \sum_{J\in\Lambda}[A_{C,A}]^{IJ,T}\{a\}^J\right], \quad I\in\lambda_H \tag{VI.36-b}$$

$$\{\Sigma\}^{B,I} = \left[C^*\right]^I \left[\sum_{J=1}^{N} [A_B]^{IJ,T}\{u\}^J + \sum_{J\in\Lambda}[A_{C,B}]^{IJ,T}\{a\}^J\right], \quad I\in\lambda_H \tag{VI.36-c}$$

Then, we use (VI.31-d,e) to rewrite (VI.34-d,e):

$$A_L[D]^L\{P^0\}^L + [D]^L[IH]^L\{K_\Sigma\}^L = \sum_{I=1}^{N}[W]^{IL,T}\{v\}^{I,L} + \sum_{I\in\Lambda}[W_C]^{IL,T}\{b\}^{I,L}, \quad L\in\lambda_C \tag{VI.36-d}$$

$$[IH]^{L,T}[D]^L\{P^0\}^L + [HDH]^L\{K_\Sigma\}^L = \sum_{I=1}^{N}[V]^{IL,T}\{v\}^{I,L} + \sum_{I\in\Lambda}[V_C]^{IL,T}\{b\}^{I,L}, L\in\lambda_C \tag{VI.36-e}$$

with

$$\left[C^*\right]^I = \frac{1}{A^I}[C]^I \quad , \qquad I=1,N \tag{VI.37}$$

From (VI.36-d,e), we can deduce $\{K_\Sigma\}^L$ and $\{P^0\}^L$:

$$\{K_\Sigma\}^L = \sum_{I=1}^{N}[M_{K\Sigma v}]^{IL}\{v\}^{I,L} + \sum_{I\in\Lambda}[M_{K\Sigma b}]^{IL}\{b\}^{I,L}, \quad L\in\lambda_C \tag{VI.38}$$

with

$$\left[M_{K\Sigma}\right]^{L} = \left[HDH\right]^{L} - \frac{1}{A_L}\left[IH\right]^{L,T}\left[D\right]^{L}\left[IH\right]^{L}, \quad L \in \lambda_C \tag{VI.39-a}$$

$$\left[M_{K\Sigma v}\right]^{IL} = \left[M_{K\Sigma}\right]^{L,-1}\left[\left[V\right]^{IL,T} - \frac{1}{A_L}\left[IH\right]^{L,T}\left[W\right]^{IL,T}\right], \quad L \in \lambda_C, \quad I = 1,N \tag{VI.39-b}$$

$$\left[M_{K\Sigma b}\right]^{IL} = \left[M_{K\Sigma}\right]^{L,-1}\left[\left[V_C\right]^{IL,T} - \frac{1}{A_L}\left[IH\right]^{L,T}\left[W_C\right]^{IL,T}\right], \quad L \in \lambda_C, \quad I \in \Lambda \tag{VI.39-c}$$

$$\left\{P^0\right\}^{L} = \sum_{I=1}^{N}\left[M_{P0v}\right]^{IL}\left\{v\right\}^{I,L} + \sum_{I\in\Lambda}\left[M_{P0b}\right]^{IL}\left\{b\right\}^{I,L}, \quad L \in \lambda_C \tag{VI.40}$$

with

$$\left[M_{P0}\right]^{L} = A_L\left[D\right]^{L} - \left[D\right]^{L}\left[IH\right]^{L}\left[HDH\right]^{L,-1}\left[IH\right]^{L,T}\left[D\right]^{L}, \quad L \in \lambda_C \tag{VI.41-a}$$

$$\left[M_{P0v}\right]^{IL} = \left[M_{P0}\right]^{L,-1}\left[\left[W\right]^{IL,T} - \left[D\right]^{L}\left[IH\right]^{L}\left[HDH\right]^{L,-1}\left[V\right]^{IL,T}\right], \quad L \in \lambda_C, \quad I = 1,N \tag{VI.41-b}$$

$$\left[M_{P0b}\right]^{IL} = \left[M_{P0}\right]^{L,-1}\left[\left[W_C\right]^{JL,T} - \left[D\right]^{L}\left[IH\right]^{L}\left[HDH\right]^{L,-1}\left[V_C\right]^{IL,T}\right], \quad L \in \lambda_C, \quad I \in \Lambda \tag{VI.41-c}$$

VI.5.2. Equilibrium equations in terms of the displacement discretization parameters

VI.5.2.1. Equilibrium equations associated with the degrees of freedom u_i^J of the cells of type *O*

$$\begin{aligned}\sum_{I=1}^{N_O}\left[A\right]^{IJ}\left\{\Sigma\right\}^{I} = &\sum_{L=1}^{N}\Big(\sum_{I=1}^{N_O}\left[A\right]^{IJ}\left[\mathrm{C}^*\right]^{I}\left[A\right]^{IL,T}\Big)\left\{u\right\}^{L} \\ &+ \sum_{L\in\Lambda}\Big(\sum_{I=1}^{N_O}\left[A\right]^{IJ}\left[\mathrm{C}^*\right]^{I}\left[A_C\right]^{IL,T}\Big)\left\{a\right\}^{L} \quad , \quad J = 1,N\end{aligned} \tag{VI.42-a}$$

$$\begin{aligned}\sum_{I\in\lambda_H}\left[A_A\right]^{IJ}\left\{\Sigma\right\}^{A,I} = &\sum_{L=1}^{N}\Big(\sum_{I\in\lambda_H}\left[A_A\right]^{IJ}\left[C^*\right]^{I}\left[A_A\right]^{IL,T}\Big)\left\{u\right\}^{L} \\ &+ \sum_{L\in\Lambda}\Big(\sum_{I\in\lambda_H}\left[A_A\right]^{IJ}\left[\mathrm{C}^*\right]^{I}\left[A_{C,A}\right]^{IL,T}\Big)\left\{a\right\}^{L} \quad , \quad J = 1,N\end{aligned} \tag{VI.42-b}$$

$$\begin{aligned}\sum_{I\in\lambda_H}\left[A_B\right]^{IJ}\left\{\Sigma\right\}^{B,I} = &\sum_{L=1}^{N}\Big(\sum_{I\in\lambda_H}\left[A_B\right]^{IJ}\left[C^*\right]^{I}\left[A_B\right]^{IL,T}\Big)\left\{u\right\}^{L} \\ &+ \sum_{L\in\Lambda}\Big(\sum_{I\in\lambda_H}\left[A_B\right]^{IJ}\left[\mathrm{C}^*\right]^{I}\left[A_{C,B}\right]^{IL,T}\Big)\left\{a\right\}^{L} \quad , \quad J = 1,N\end{aligned} \tag{VI.42-c}$$

$$\begin{aligned}
&[W]^{JL}\{P^0\}^L+[V]^{JL}\{K_\Sigma\}^L=\\
&\quad[W]^{JL}\left[\sum_{I=1}^{N}[M_{P0v}]^{IL}\{v\}^{IL}+\sum_{I\in\Lambda}[M_{P0b}]^{IL}\{b\}^{IL}\right]\\
&\quad+[V]^{JL}\left[\sum_{I=1}^{N}[M_{K\Sigma v}]^{IL}\{v\}^{IL}+\sum_{I\in\Lambda}[M_{K\Sigma b}]^{IL}\{b\}^{IL}\right],\quad J=1,N\quad L\in\lambda_C\\
&[W]^{JL}\{P^0\}^L+[V]^{JL}\{K_\Sigma\}^L=\\
&\quad\left[\sum_{I=1}^{N}[S_v^O]^{IJL}\{v\}^{IL}+\sum_{I\in\Lambda}[S_b^O]^{IJL}\{b\}^{IL}\right],\quad J=1,N\quad L\in\lambda_C
\end{aligned}\tag{VI.42-d}$$

with

$$[S_v^O]^{IJL}=[W]^{JL}[M_{P0v}]^{IL}+[V]^{JL}[M_{K\Sigma v}]^{IL}\tag{VI.42-e}$$

$$[S_b^O]^{IJL}=[W]^{JL}[M_{P0b}]^{IL}+[V]^{JL}[M_{K\Sigma b}]^{IL}\tag{VI.42-f}$$

$$[W]^{JL}[M_{P0v}]^{IL}=[W]^{JL}[M_{P0}]^{L,-1}\left[[W]^{IL,T}-[D]^L[IH]^L[HDH]^{L,-1}[V]^{IL,T}\right]\tag{VI.42-g}$$

$$[W]^{JL}[M_{P0b}]^{IL}=[W]^{JL}[M_{P0}]^{L,-1}\left[[W_C]^{IL,T}-[D]^L[IH]^L[HDH]^{L,-1}[V_C]^{IL,T}\right]\tag{VI.42-h}$$

$$[V]^{JL}[M_{K\Sigma v}]^{IL}=[V]^{JL}[M_{K\Sigma}]^{L,-1}\left[[V]^{IL,T}-\frac{1}{A_L}[IH]^{L,T}[W]^{IL,T}\right]\tag{VI.42-i}$$

$$[V]^{JL}[M_{K\Sigma b}]^{IL}=[V]^{JL}[M_{K\Sigma}]^{L,-1}\left[[V_C]^{IL,T}-\frac{1}{A_L}[IH]^{L,T}[W_C]^{IL,T}\right]\tag{VI.42-i}$$

$$\begin{aligned}
&\sum_{L\in\lambda_C}[R]^{L,T}\left[[W]^{JL}\{P^0\}^L+[V]^{JL}\{K_\Sigma\}^L\right]=\\
&\quad\sum_{L\in\lambda_C}[R]^{L,T}\left[\sum_{I=1}^{N}[S_v^O]^{IJL}\{v\}^{I,L}+\sum_{I\in\Lambda}[S_b^O]^{IJL}\{b\}^{I,L}\right],\quad J=1,N
\end{aligned}\tag{VI.42-k}$$

Let us define the following sub-matrices

$$[M_O^O]^{JL}=\sum_{I=1}^{N_O}[A]^{IJ}\left[\mathrm{C}^*\right]^I[A]^{IL,T},\quad J=1,N,\quad L=1,N\tag{VI.43-a}$$

$$[M_O^C]^{JL}=\sum_{I=1}^{N_O}[A]^{IJ}\left[\mathrm{C}^*\right]^I[A_C]^{IL,T},\quad J=1,N,\quad L\in\Lambda\tag{VI.43-b}$$

$$[M_A^A]^{JL}=\sum_{I\in\lambda_H}[A_A]^{IJ}\left[\mathrm{C}^*\right]^I[A_A]^{IL,T},\quad J=1,N,\quad L=1,N\tag{VI.44-a}$$

$$\left[M_A^{C,A}\right]^{JL} = \sum_{I\in\lambda_H}\left[A_A\right]^{IJ}\left[\mathrm{C}^*\right]^{I}\left[A_{C,A}\right]^{IL,T}, \quad J=1,N\,, \quad L\in\Lambda \tag{VI.44-b}$$

$$\left[M_B^{B}\right]^{JL} = \sum_{I\in\lambda_H}\left[A_B\right]^{IJ}\left[\mathrm{C}^*\right]^{I}\left[A_{B}\right]^{IL,T}, \quad J=1,N\,, \quad L=1,N \tag{VI.45-a}$$

$$\left[M_B^{C,B}\right]^{JL} = \sum_{I\in\lambda_H}\left[A_B\right]^{IJ}\left[\mathrm{C}^*\right]^{I}\left[A_{C,B}\right]^{IL,T}, \quad J=1,N\,, \quad L\in\Lambda \tag{VI.45-b}$$

$$\left[M_W^{W}\right]^{JI} = \sum_{L\in\lambda_C}\left[R\right]^{L,T}\left[S_v^{O}\right]^{I\,JL}\left[R\right]^{L}, \quad J=1,N\,, \quad I=1,N \tag{VI.46-a}$$

$$\left[M_W^{W,C}\right]^{JI} = \sum_{L\in\lambda_C}\left[R\right]^{L,T}\left[S_b^{O}\right]^{I\,JL}\left[R\right]^{L}, \quad J=1,N\,, \quad I\in\Lambda \tag{VI.46-b}$$

Hence, equations (VI.42-a,b,c,k) become

$$\sum_{I=1}^{N_O}\left[A\right]^{IJ}\left\{\Sigma\right\}^{I} = \sum_{L=1}^{N}\left[M_O^{O}\right]^{JL}\left\{u\right\}^{L} + \sum_{L\in\Lambda}\left[M_O^{C}\right]^{JL}\left\{a\right\}^{L} \quad , \quad J=1,N \tag{VI.47-a}$$

$$\sum_{I=1}^{N_O}\left[A_A\right]^{IJ}\left\{\Sigma\right\}^{A,I} = \sum_{L=1}^{N}\left[M_A^{A}\right]^{JL}\left\{u\right\}^{L} + \sum_{L\in\Lambda}\left[M_A^{C,A}\right]^{JL}\left\{a\right\}^{L}, \quad J=1,N \tag{VI.47-b}$$

$$\sum_{I=1}^{N_O}\left[A_B\right]^{IJ}\left\{\Sigma\right\}^{B,I} = \sum_{L=1}^{N}\left[M_B^{B}\right]^{JL}\left\{u\right\}^{L} + \sum_{L\in\Lambda}\left[M_B^{C,B}\right]^{JL}\left\{a\right\}^{L} \quad , \quad J=1,N \tag{VI.47-c}$$

$$\begin{aligned}\sum_{L\in\lambda_C}\left[R\right]^{L,T}\left[\left[W\right]^{JL}\left\{P^0\right\}^{L} + \left[V\right]^{JL}\left\{K_\Sigma\right\}^{L}\right] = \\ \sum_{L=1}^{N}\left[M_W^{W}\right]^{JL}\left\{u\right\}^{L} + \sum_{L\in\Lambda}\left[M_W^{W,C}\right]^{JL}\left\{a\right\}^{L} \quad , \quad J=1,N\end{aligned} \tag{VI.47-d}$$

Then the equilibrium equation (VI.32) becomes

$$\begin{aligned}&\sum_{L=1}^{N}\left[M_{UU}\right]^{JL}\left\{u\right\}^{L} + \sum_{L\in\Lambda}\left[M_{UA}\right]^{JL}\left\{a\right\}^{L} \\ &-\left\{\sum_{K=1}^{M_u^O} B^{KJ}\left\{r\right\}^{K} + \sum_{K=1}^{M_u^A} B^{KJ}\left\{r\right\}^{A(K)} + \sum_{K=1}^{M_u^B} B^{KJ}\left\{r\right\}^{B(K)}\right\} = \left\{\widetilde{Q}\right\}^{J} \quad , \quad J=1,N\end{aligned} \tag{VI.48}$$

with

$$\left[M_{UU}\right]^{JL} = \left[M_O^{O}\right]^{JL} + \left[M_A^{A}\right]^{JL} + \left[M_B^{B}\right]^{JL} + \left[M_W^{W}\right]^{JL}, J=1,N \quad L=1,N \tag{VI.49-a}$$

$$\left[M_{UA}\right]^{JL} = \left[M_O^{C}\right]^{JL} + \left[M_A^{C,A}\right]^{JL} + \left[M_B^{C,B}\right]^{JL} + \left[M_W^{W,C}\right]^{JL}, J=1,N \quad L\in\Lambda \tag{VI.49-b}$$

$$\left\{\widetilde{Q}\right\}^{J} = \sum_{I=1}^{N}\left\{\widetilde{F}\right\}^{IJ} + \sum_{K=1}^{M_t}\left\{\widetilde{T}\right\}^{KJ} \tag{VI.49-d}$$

VI.5.2.2. Equilibrium equations associated with the degrees of freedom a_i^J of the cells of type *H* and *C*

$$\sum_{I=1}^{N_O}[A_C]^{IJ}\{\Sigma\}^I=\sum_{L=1}^{N}(\sum_{I=1}^{N_O}[A_C]^{IJ}\left[\mathrm{C}^*\right]^I[A]^{IL,T})\{u\}^L + \sum_{L\in\Lambda}(\sum_{I=1}^{N_O}[A_C]^{IJ}\left[\mathrm{C}^*\right]^I[A_C]^{IL,T})\{a\}^L \quad , \quad J\in\Lambda \tag{VI.50-a}$$

$$\sum_{I\in\lambda_H}[A_{C,A}]^{IJ}\{\Sigma\}^{A,I}=\sum_{L=1}^{N}(\sum_{I\in\lambda_H}[A_{C,A}]^{IJ}\left[C^*\right]^I[A_A]^{IL,T})\{u\}^L + \sum_{L\in\Lambda}(\sum_{I\in\lambda_H}[A_{C,A}]^{IJ}\left[\mathrm{C}^*\right]^I[A_{C,A}]^{IL,T})\{a\}^L \quad , \quad J\in\Lambda \tag{VI.50-b}$$

$$\sum_{I\in\lambda_H}[A_{C,B}]^{IJ}\{\Sigma\}^{B,I}=\sum_{L=1}^{N}(\sum_{I\in\lambda_H}[A_{C,B}]^{IJ}\left[C^*\right]^I[A_B]^{IL,T})\{u\}^L + \sum_{L\in\Lambda}(\sum_{I\in\lambda_H}[A_{C,B}]^{IJ}\left[\mathrm{C}^*\right]^I[A_{C,B}]^{IL,T})\{a\}^L \quad , \quad J\in\Lambda \tag{VI.50-c}$$

$$\begin{aligned}&[W_C]^{JL}\{P^0\}^L+[V_C]^{JL}\{K_\Sigma\}^L=\\ &\quad[W_C]^{JL}\left[\sum_{I=1}^{N}[M_{P0v}]^{IL}\{v\}^{IL}+\sum_{I\in\Lambda}[M_{P0b}]^{IL}\{b\}^{IL}\right]\\ &+[V_C]^{JL}\left[\sum_{I=1}^{N}[M_{K\Sigma v}]^{IL}\{v\}^{IL}+\sum_{I\in\Lambda}[M_{K\Sigma b}]^{IL}\{b\}^{IL}\right],\quad J\in\Lambda\quad L\in\lambda_C\\ &[W_C]^{JL}\{P^0\}^L+[V_C]^{JL}\{K_\Sigma\}^L=\\ &\quad\left[\sum_{I=1}^{N}[S_v^\Lambda]^{IJL}\{v\}^{I,L}+\sum_{I\in\Lambda}[S_b^\Lambda]^{IJL}\{b\}^{I,L}\right],\quad J\in\Lambda\quad L\in\lambda_C\end{aligned} \tag{VI.50-d}$$

with

$$[S_v^\Lambda]^{IJL}=[W_C]^{JL}[M_{P0v}]^{IL}+[V_C]^{JL}[M_{K\Sigma v}]^{IL}\ ,\quad J\in\Lambda\quad L\in\lambda_C\quad I=1,N \tag{VI.50-e}$$

$$[S_b^\Lambda]^{IJL}=[W_C]^{JL}[M_{P0b}]^{IL}+[V_C]^{JL}[M_{K\Sigma b}]^{IL}\ ,\quad J\in\Lambda\quad L\in\lambda_C\quad I\in\Lambda \tag{VI.50-f}$$

$$\begin{aligned}&\sum_{L\in\lambda_C}[R]^{L,T}\left[[W]^{JL}\{P^0\}^L+[V]^{JL}\{K_\Sigma\}^L\right]=\\ &\quad\sum_{L\in\lambda_C}[R]^{L,T}\left[\sum_{I=1}^{N}[S_v^\Lambda]^{IJL}\{v\}^{IL}+\sum_{I\in\Lambda}[S_b^\Lambda]^{IJL}\{b\}^{IL}\right],\quad J\in\Lambda\end{aligned} \tag{VI.50-h}$$

Let us define the following sub-matrices

$$\left[M_C^O\right]^{JL} = \sum_{I=1}^{N_O} \left[A_C\right]^{IJ} \left[\mathrm{C}^*\right]^I \left[A\right]^{IL,T}, \quad J \in \Lambda, \quad L = 1, N \tag{VI.51-a}$$

$$\left[M_C^C\right]^{JL} = \sum_{I=1}^{N_O} \left[A_C\right]^{IJ} \left[\mathrm{C}^*\right]^I \left[A_C\right]^{IL,T}, \quad J \in \Lambda, \quad L \in \Lambda \tag{VI.51-b}$$

$$\left[M_{C,A}^A\right]^{JL} = \sum_{I \in \lambda_H} \left[A_{C,A}\right]^{IJ} \left[\mathrm{C}^*\right]^I \left[A_A\right]^{IL,T}, \quad J \in \Lambda, \quad L = 1, N \tag{VI.52-a}$$

$$\left[M_{C,A}^{C,A}\right]^{JL} = \sum_{I \in \lambda_H} \left[A_{C,A}\right]^{IJ} \left[\mathrm{C}^*\right]^I \left[A_{C,A}\right]^{IL,T}, \quad J \in \Lambda, \quad L \in \Lambda \tag{VI.52-b}$$

$$\left[M_{C,B}^B\right]^{JL} = \sum_{I \in \lambda_H} \left[A_{C,B}\right]^{IJ} \left[\mathrm{C}^*\right]^I \left[A_B\right]^{IL,T}, \quad J \in \Lambda, \quad L = 1, N \tag{VI.53-a}$$

$$\left[M_{C,B}^{C,B}\right]^{JL} = \sum_{I \in \lambda_H} \left[A_{C,B}\right]^{IJ} \left[\mathrm{C}^*\right]^I \left[A_{C,B}\right]^{IL,T}, \quad J \in \Lambda, \quad L \in \Lambda \tag{VI.53-b}$$

$$\left[M_{W,C}^W\right]^{JI} = \sum_{L \in \lambda_C} \left[R\right]^{L,T} \left[S_v^\Lambda\right]^{IJL} \left[R\right]^L, \quad J \in \Lambda, \quad I = 1, N \tag{VI.54-a}$$

$$\left[M_{W,C}^{W,C}\right]^{JI} = \sum_{L \in \lambda_C} \left[R\right]^{L,T} \left[S_b^\Lambda\right]^{IJL} \left[R\right]^L, \quad J \in \Lambda, \quad I \in \Lambda \tag{VI.54-b}$$

Hence, equations (VI.50) become

$$\sum_{I=1}^{N_O} \left[A_C\right]^{IJ} \left\{\Sigma\right\}^I = \sum_{L=1}^{N} \left[M_C^O\right]^{JL} \left\{u\right\}^L + \sum_{L \in \Lambda} \left[M_C^C\right]^{JL} \left\{a\right\}^L \quad , \quad J \in \Lambda \tag{VI.55-a}$$

$$\sum_{I=1}^{N_O} \left[A_{C,A}\right]^{IJ} \left\{\Sigma\right\}^{A,I} = \sum_{L=1}^{N} \left[M_{C,A}^A\right]^{JL} \left\{u\right\}^L + \sum_{L \in \Lambda} \left[M_{C,A}^{C,A}\right]^{JL} \left\{a\right\}^L \quad , \quad J \in \Lambda \tag{VI.55-b}$$

$$\sum_{I=1}^{N_O} \left[A_{C,B}\right]^{IJ} \left\{\Sigma\right\}^{B,I} = \sum_{L=1}^{N} \left[M_{C,B}^B\right]^{JL} \left\{u\right\}^L + \sum_{L \in \Lambda} \left[M_{C,B}^{C,B}\right]^{JL} \left\{a\right\}^L \quad , \quad J \in \Lambda \tag{VI.55-c}$$

$$\begin{aligned} &\sum_{L \in \lambda_C} \left[R\right]^{L,T} \left[\left[W_C\right]^{JL} \left\{P^0\right\}^L + \left[V_C\right]^{JL} \left\{K_\Sigma\right\}^L\right] = \\ &\qquad \sum_{L=1}^{N} \left[M_{W,C}^W\right]^{JL} \left\{u\right\}^L + \sum_{L \in \Lambda} \left[M_{W,C}^{W,C}\right]^{JL} \left\{a\right\}^L \quad , \quad J = 1, N \end{aligned} \tag{VI.55-d}$$

Then the equilibrium equation (VI.33) becomes

$$\begin{aligned} &\sum_{L=1}^{N} \left[M_{AU}\right]^{JL} \left\{u\right\}^L + \sum_{L \in \Lambda} \left[M_{AA}\right]^{JL} \left\{a\right\}^L \\ &\quad - \left\{ \sum_{K=1}^{M_u^O} B_C^{KJ} \left\{r\right\}^K + \sum_{K=1}^{M_u^A} B_C^{KJ} \left\{r\right\}^{A(K)} + \sum_{K=1}^{M_u^B} B_C^{KJ} \left\{r\right\}^{B(K)} \right\} = \left\{\widetilde{Q}_C\right\}^J \quad , \quad J \in \Lambda \end{aligned} \tag{VI.56}$$

with

$$\left[M_{AU}\right]^{JL} = \left[M_C^O\right]^{JL} + \left[M_{C,A}^A\right]^{JL} + \left[M_{C,B}^B\right]^{JL} + \left[M_{W,C}^W\right]^{JL}, J \in \Lambda \quad L = 1, N \tag{VI.57-a}$$

$$\left[M_{AA}\right]^{JL} = \left[M_C^C\right]^{JL} + \left[M_{C,A}^{C,A}\right]^{JL} + \left[M_{C,B}^{C,B}\right]^{JL} + \left[M_{W,C}^{W,C}\right]^{JL}, J \in \Lambda \quad L \in \Lambda \tag{VI.57-b}$$

$$\left\{\widetilde{Q}_C\right\}^J = \sum_{I=1}^{N} \left\{\widetilde{F}_C\right\}^{IJ} + \sum_{K=1}^{M_t} \left\{\widetilde{T}_C\right\}^{IJ}$$

VI.5.3. Summary of the equations

In order to summarize the results, several tables are given below.

The main variables are collected in table VI.2.

The degrees of freedom of the discretization are collected in table VI.3.

The interpolation functions are collected in table VI.4.

The scalars appearing in the equations are collected in table VI.5.

The matrices appearing in the equations are collected in table VI.6.

The discretized equations deduced from the FdV variational principle are collected in table VI.7.

Table VI.2. Main variables	
Reference frames	
(X_1, X_2)	Global frame (X_1, X_2) of the two-dimensional solid
$(Y_1, Y_2)^L$, $L \in \lambda_C$	Local frame associated with the crack tip L
Variables associated with the cells	
N^O, N^H, N^C,	Number of cells of types O, H and C respectively
$N = N^O + N^H + N^C$	Total number of nodes
M_u^O	Number of edges of cells of type O on which support reactions exist
M_u^A or M_u^B	Number of edges $A(K)$ or $B(K)$, belonging to the parts A or B of a cell of type H, on which support reactions exist
λ_H	The set of cells of type H
λ_C	The set of cells of type C
$\Lambda = \lambda_H \cup \lambda_C$	The set of crack nodes
A_I , $I = 1, N^O$ and $I \in \lambda_C$	Area of a cell I of type O or type C
$A_{A,I}$ or $A_{B,I}$, $I \in \lambda_H$	Area of the parts A or B of a cell I of type H
C_I , $I = 1, N^O$ and $I \in \lambda_C$	Contour of a cell I of type O or C, oriented clockwise
$C_{A(I)}$ or $C_{B(I)}$, $I \in \lambda_H$	Contour of the parts A or B of a cell I of type H, oriented clockwise
N_j^I , $I = 1, N^O$ and $I \in \lambda_C$	Outside normal to C_I expressed in the global frame (X_1, X_2)
M_j^L , $L \in \lambda_C$	Outside normal to C_L expressed in the local frame $(Y_1, Y_2)^L$

Table VI.3. Degrees of freedom of the discretization.	
Assumed stresses	
$\{\Sigma\}^I = \begin{Bmatrix} \Sigma_{11}^I \\ \Sigma_{22}^I \\ \Sigma_{12}^I \end{Bmatrix}, \quad I = 1, N^O$	Stresses, expressed in the global frame (X_1, X_2), in the cells of type O
$\{\Sigma\}^{I,A} = \begin{Bmatrix} \Sigma_{11}^{I,A} \\ \Sigma_{22}^{I,A} \\ \Sigma_{12}^{I,A} \end{Bmatrix}, \quad \{\Sigma\}^{I,B} = \begin{Bmatrix} \Sigma_{11}^{I,B} \\ \Sigma_{22}^{I,B} \\ \Sigma_{12}^{I,B} \end{Bmatrix}, \quad I \in \lambda_H$	Stresses, expressed in the global frame (X_1, X_2), in the parts A and B of the cells of type H
$\{P^0\}^L = \begin{Bmatrix} P_{11}^{0L} \\ P_{22}^{0L} \\ P_{12}^{0L} \end{Bmatrix}, \quad L \in \lambda_C$	Constant part of the stresses, expressed in the local frame $(Y_1, Y_2)^L$, in the cells of type C
Assumed strains	
$\{\varepsilon\}^I = \begin{Bmatrix} \varepsilon_{11}^I \\ \varepsilon_{22}^I \\ \varepsilon_{12}^I \end{Bmatrix}, \quad I = 1, N^O$	Strains, expressed in the global frame (X_1, X_2), in the cells of type O
$\{\varepsilon\}^{I,A} = \begin{Bmatrix} \varepsilon_{11}^{I,A} \\ \varepsilon_{22}^{I,A} \\ \varepsilon_{12}^{I,A} \end{Bmatrix}, \quad \{\varepsilon\}^{I,B} = \begin{Bmatrix} \varepsilon_{11}^{I,B} \\ \varepsilon_{22}^{I,B} \\ \varepsilon_{12}^{I,B} \end{Bmatrix}, \quad I \in \lambda_H$	Strains, expressed in the global frame (X_1, X_2), in the parts A and B of the cells of type H
$\{\gamma^0\}^L = \begin{Bmatrix} \gamma_{11}^{0L} \\ \gamma_{22}^{0L} \\ 2\gamma_{12}^{0L} \end{Bmatrix}, \quad L \in \lambda_C$	Constant part of the strains, expressed in the local frame $(Y_1, Y_2)^L$, in the cells of type C
Assumed displacements	
$\{u\}^I = \begin{Bmatrix} u_1^I \\ u_2^I \end{Bmatrix}, \quad I = 1, N$	Displacements of a node I, expressed in (X_1, X_2)
$\{v\}^{I,L} = \begin{Bmatrix} v_1^{I,L} \\ v_2^{I,L} \end{Bmatrix}, \quad I = 1, N$	Displacements of a node I, expressed in $(Y_1, Y_2)^L$
$\{a\}^I = \begin{Bmatrix} a_1^I \\ a_2^I \end{Bmatrix}, \quad I \in \Lambda$	Additional DOF, expressed in (X_1, X_2), of a node $I \in \Lambda$
$\{b\}^{I,L} = \begin{Bmatrix} b_1^{I,L} \\ b_2^{I,L} \end{Bmatrix}, \quad I \in \Lambda$	Additional DOF, expressed in $(Y_1, Y_2)^L$, of a node $I \in \Lambda$
Crack tip parameters	
$\{K_\Sigma\}^L = \begin{Bmatrix} K_{\Sigma 1}^L \\ K_{\Sigma 2}^L \end{Bmatrix}, \quad L \in \lambda_C$	Parameters (with the meaning of a stress intensity factor) associated with each crack tip
Assumed support reactions	

$\{r\}^K = \begin{Bmatrix} r_1^K \\ r_2^K \end{Bmatrix}, \quad K = 1, M_u^O$	Support reactions on the edge K of a cell of type O
$\{r\}^{A(K)} = \begin{Bmatrix} r_1^{A(K)} \\ r_2^{A(K)} \end{Bmatrix}, K = 1, M_u^A \;\; ; \;\; \{r\}^{B(K)} = \begin{Bmatrix} r_1^{B(K)} \\ r_2^{B(K)} \end{Bmatrix}, \quad K = 1, M_u^B$	Support reactions on the edges $A(K)$ or $B(K)$ belonging to the parts A or B of a cell of type H

Table VI.4. Interpolation functions

$C(\underline{X})$	Crack function
$\Phi_J, \quad I = 1, N$	Laplace interpolant associated with node (or cell) J
$\{H_1\}^L = \begin{Bmatrix} H_{11}^L \\ H_{12}^L \\ H_{13}^L \end{Bmatrix} = \frac{1}{\sqrt{2\pi r_L}} \cos\frac{\theta_L}{2} \begin{Bmatrix} 1 - \sin\frac{\theta_L}{2} \sin\frac{3\theta_L}{2} \\ 1 + \sin\frac{\theta_L}{2} \sin\frac{3\theta_L}{2} \\ -\sin\frac{\theta_L}{2} \cos\frac{3\theta_L}{2} \end{Bmatrix}, \quad L \in \lambda_C$ $\{H_2\}^L = \begin{Bmatrix} H_{21}^L \\ H_{22}^L \\ H_{23}^L \end{Bmatrix} = \frac{1}{\sqrt{2\pi r_L}} \begin{Bmatrix} \sin\frac{\theta_L}{2}(2 + \cos\frac{\theta_L}{2} \cos\frac{3\theta_L}{2}) \\ -\cos\frac{\theta_L}{2}\sin\frac{\theta_L}{2} \cos\frac{3\theta_L}{2} \\ \cos\frac{\theta_L}{2}(1 - \sin\frac{\theta_L}{2} \sin\frac{3\theta_L}{2}) \end{Bmatrix}, \quad L \in \lambda_C$	Stress interpolation functions for mode 1 and mode 2 fractures associated with the crack tip L, expressed in the local frame $(Y_1, Y_2)^L$

Table VI.5. Scalars appearing in the equations

Scalar	Comments
$A_j^{IJ} = \oint_{C_I} N_j^I \Phi_J \, dC_I, \quad I = 1, N^O, \; J = 1, N$	C_I is the contour of cell I, oriented clockwise
$A_{Aj}^{IJ} = \oint_{C_{A(I)}} N_j^I \Phi_J \, dC_{A(I)}, \;\; A_{Bj}^{IJ} = \oint_{C_{A(I)}} N_j^I \Phi_J \, dC_{B(I)}, \quad I \in \lambda_H, \; J = 1, N$	$C_{A(I)}$ and $C_{B(I)}$ are the contours of the parts A and B of cell I, oriented clockwise
$A_{Cj}^{IJ} = \oint_{C_I} N_j^I \, C(X) \Phi_J \, dC_I, \quad I = 1, N^O, \; J \in \Lambda$	C_I is the contour of cell I, oriented clockwise
$A_{C,Aj}^{IJ} = \oint_{C_{A(I)}} N_j^I \, C(X) \Phi_J \, dC_{A(I)}, \;\; A_{C,Bj}^{IJ} = \oint_{C_{B(I)}} N_j^I \, C(X) \Phi_J \, dC_{B(I)} \quad I \in \lambda_H, \; J \in \Lambda$	$C_{A(I)}$ and $C_{B(I)}$ are the contours of the parts A and B of cell I, oriented clockwise
$B^{KJ} = \int_{S_K} \Phi_J \, dS_K, \quad J = 1, N$	S_K is an edge of a cell on which a support reaction exists
$B_C^{KJ} = \int_{S_K} C(\underline{X}) \Phi_J \, dS_K, \quad J \in \Lambda$	

$\widetilde{F}_i^{IJ} = \int_{A_I} F_i \Phi_J dA_I , \quad I = 1, N , \; J = 1, N$	A_I is the area of a cell I on which body forces F_i are imposed
$\widetilde{F}_{C,i}^{IJ} = \int_{A_I} C(\underline{X})\, F_i \; \Phi_J dA_I , \quad I = 1, N , \; J \in \Lambda$	
$\widetilde{T}_i^{KJ} = \int_{S_K} T_i \, \Phi_J dS_K , \quad K = 1, M_t , \quad J = 1, N$	S_K is an edge of a cell on which surface tractions T_i are imposed; M_t is the number of edges (of any type of cells) on which surface tractions T_i are imposed
$\widetilde{T}_{C,i}^{KJ} = \int_{S_K} C(\underline{X})\, T_i \; \Phi_J dS_K , \quad K = 1, M_t , \; J \in \Lambda$	
$\widetilde{U}_i^K = \int_{S_K} \widetilde{u}_i \, dS_K \quad K = 1, N^O$	S_K is an edge of a cell of type O on which displacements $\widetilde{u}_i$ are imposed
$\widetilde{U}_i^{A(K)} = \int_{S_K} \widetilde{u}_i^{A(K)} dS_K ; \quad \widetilde{U}_i^{B(K)} = \int_{S_K} \widetilde{u}_i^{B(K)} dS_K \quad K \in \lambda_H$	S_K is an edge belonging to part A or part B of a cell of type H on which displacements $\widetilde{u}_i^A$ or $\widetilde{u}_i^B$ are imposed

Table VI.6. Matrices appearing in the equations

$$[A]^{IJ} = \begin{bmatrix} A_1^{IJ} & 0 & A_2^{IJ} \\ 0 & A_2^{IJ} & A_1^{IJ} \end{bmatrix}, \quad I = 1, N^O , \; J = 1, N$$

$$[A_A]^{IJ} = \begin{bmatrix} A_{A1}^{IJ} & 0 & A_{A2}^{IJ} \\ 0 & A_{A2}^{IJ} & A_{A1}^{IJ} \end{bmatrix}, \quad I \in \lambda_H , \; J = 1, N$$

$$[A_B]^{IJ} = \begin{bmatrix} A_{B1}^{IJ} & 0 & A_{B2}^{IJ} \\ 0 & A_{B2}^{IJ} & A_{B1}^{IJ} \end{bmatrix}, \quad I \in \lambda_H , \; J = 1, N$$

$$[A_C]^{IJ} = \begin{bmatrix} A_{C1}^{IJ} & 0 & A_{C2}^{IJ} \\ 0 & A_{C2}^{IJ} & A_{C1}^{IJ} \end{bmatrix}, \quad I = 1, N^O , \; J \in \Lambda$$

$$[A_{C,A}]^{IJ} = \begin{bmatrix} A_{C,A1}^{IJ} & 0 & A_{C,A2}^{IJ} \\ 0 & A_{C,A1}^{IJ} & A_{C,A1}^{IJ} \end{bmatrix}, \quad I \in \lambda_H , \; J \in \Lambda$$

$$[A_{C,B}]^{IJ} = \begin{bmatrix} A_{C,B1}^{IJ} & 0 & A_{C,B2}^{IJ} \\ 0 & A_{C,B1}^{IJ} & A_{C,B1}^{IJ} \end{bmatrix}, \quad I \in \lambda_H , \; J \in \Lambda$$

$$[C]^L = \frac{E_L^*}{(1+\nu_L^*)(1-\nu_L^*)} \begin{bmatrix} 1 & \nu_L^* & 0 \\ \nu_L^* & 1 & 0 \\ 0 & 0 & \dfrac{1-\nu_L^*}{2} \end{bmatrix} ; \quad [D]^L = \frac{1}{E_L^*} \begin{bmatrix} 1 & -\nu_L^* & 0 \\ -\nu_L^* & 1 & 0 \\ 0 & 0 & 2(1+\nu_L^*) \end{bmatrix}$$

$$E_L^* = \frac{E_L}{1-\nu_L^2} \text{ in plane strain state} \quad \text{or} \quad E_L^* = E_L \text{ in plane stress state}, \qquad L = 1, N$$

$$\nu_L^* = \frac{\nu_L}{1-\nu_L} \text{ in plane strain state} \quad \text{or} \quad \nu_L^* = \nu_L \text{ in plane stress state}, \qquad L = 1, N$$

$$\left\{\widetilde{F}\right\}^{IJ} = \begin{Bmatrix} \widetilde{F}_1^{IJ} \\ \widetilde{F}_2^{IJ} \end{Bmatrix}, \quad I = 1, N, \; J = 1, N$$

$$\left\{\widetilde{F}_C\right\}^{IJ} = \begin{Bmatrix} \widetilde{F}_{C1}^{IJ} \\ \widetilde{F}_{C2}^{IJ} \end{Bmatrix}, \quad I = 1, N, \; J \in \Lambda$$

$$\left[HDH\right]^L = \begin{bmatrix} \int\limits_{A_L} \langle H_1 \rangle^L [D]^L \{H_1\}^L \, dA_L & \int\limits_{A_L} \langle H_1 \rangle^L [D]^L \{H_2\}^L \, dA_L \\ \int\limits_{A_L} \langle H_2 \rangle^L [D]^L \{H_1\}^L \, dA_L & \int\limits_{A_L} \langle H_2 \rangle^L [D]^L \{H_2\}^L \, dA_L \end{bmatrix}, \quad L \in \lambda_C$$

$$\left[IH\right]^L = \begin{bmatrix} \int\limits_{A_L} \{H_1\}^L \, dA_L & \int\limits_{A_L} \{H_2\}^L \, dA_L \end{bmatrix}, \quad L \in \lambda_C$$

$$\left[M\right]^L = \begin{bmatrix} M_1^L & 0 & M_2^L \\ 0 & M_2^L & M_1^L \end{bmatrix}, \quad L \in \lambda_C$$

$$\left\{\widetilde{T}\right\}^{KJ} = \begin{Bmatrix} \widetilde{T}_1^{KJ} \\ \widetilde{T}_2^{KJ} \end{Bmatrix}, \quad K = 1, M_t, \quad J = 1, N$$

$$\left\{\widetilde{T}_C\right\}^{KJ} = \begin{Bmatrix} \widetilde{T}_{C1}^{KJ} \\ \widetilde{T}_{C2}^{KJ} \end{Bmatrix}, \quad K = 1, M_t, \; J \in \Lambda$$

$$\left\{\widetilde{U}\right\}^{K} = \begin{Bmatrix} \widetilde{U}_1^{K} \\ \widetilde{U}_2^{K} \end{Bmatrix}, \quad K = 1, N^O$$

$$\left\{\widetilde{U}\right\}^{A(K)} = \begin{Bmatrix} \widetilde{U}_1^{A(K)} \\ \widetilde{U}_2^{A(K)} \end{Bmatrix} \; ; \; \left\{\widetilde{U}\right\}^{B(K)} = \begin{Bmatrix} \widetilde{U}_1^{B(K)} \\ \widetilde{U}_2^{B(K)} \end{Bmatrix}, \quad K \in \lambda_H$$

$$\left[V\right]^{JL} = \begin{bmatrix} \int\limits_{C_L} \Phi_J \left[M\right]^L \{H_1\}^L \, dC_L & \int\limits_{C_L} \Phi_J \left[M\right]^L \{H_2\}^L \, dC_L \end{bmatrix}, \quad J = 1, N \;\; , \;\; L \in \lambda_C$$

$$\left[V_C\right]^{JL} = \begin{bmatrix} \int\limits_{C_L} C(\underline{X}) \Phi_J \left[M\right]^L \{H_1\}^L \, dC_L & \int\limits_{C_L} C(\underline{X}) \Phi_J \left[M\right]^L \{H_2\}^L \, dC_L \end{bmatrix}, J \in \Lambda, L \in \lambda_C$$

$$\left[W\right]^{JL} = \int\limits_{C_L} \Phi_J \left[M\right]^L dC_L \;\; , \;\; J = 1, N, \; L \in \lambda_C$$

$$\left[W_C\right]^{JL} = \int\limits_{C_L} C(\underline{X}) \Phi_J \left[M\right]^L dC_L \;\; , \;\; J \in \Lambda, \; L \in \lambda_C$$

Table VI.7. Discretized equations in matrix form for the XNEM

Equations	Comments	
$\{\Sigma\}^I = \{\sigma\}^I = [C]^I \{\varepsilon\}^I, \quad I = 1, N_O$	Constitutive stresses in cells of type O	(VI.31-a)
$\{\Sigma\}^{A,J} = \{\sigma\}^{A,J} = [C]^J \{\varepsilon\}^{A,J}, \quad J \in \lambda_H$	Constitutive stresses in cells of type H	(VI.31-b)
$\{\Sigma\}^{B,J} = \{\sigma\}^{B,J} = [C]^J \{\varepsilon\}^{B,J}, \quad J \in \lambda_H$		(VI.31-c)
$\{P^0\}^L = [C]^L \{\gamma^0\}^L, \quad L \in \lambda_C$	Constitutive stresses in cells of type C	(VI.31-d)
$A_I \{\varepsilon\}^I = \sum_{J=1}^{N} [A]^{IJ,T} \{u\}^J + \sum_{J \in \Lambda} [A_C]^{IJ,T} \{a\}^J, \quad I = 1, N_O$	Compatibility equation for cells of type O	(VI.34-a)
$A_{A,I} \{\varepsilon\}^{A,I} = \sum_{J=1}^{N} [A_A]^{IJ,T} \{u\}^J + \sum_{J \in \Lambda} [A_{C,A}]^{IJ,T} \{a\}^J, \quad I \in \lambda_H$	Compatibility equation for cells of type H	(VI.34-b)
$A_{B,I} \{\varepsilon\}^{B,I} = \sum_{J=1}^{N} [A_B]^{IJ,T} \{u\}^J + \sum_{J \in \Lambda} [A_{C,B}]^{IJ,T} \{a\}^J, \quad I \in \lambda_H$		(VI.34-c)
$A_L \{\gamma^0\}^L + [D]^L [IH]^L \{K_\varepsilon\}^L = \sum_{I=1}^{N} [W]^{IL,T} \{v\}^{I,L} + \sum_{I \in \Lambda} [W_C]^{IL,T} \{b\}^{I,L}, \quad L \in \lambda_C$	Compatibility equation for cells of type C	(VI.34-d)
$[IH]^{L,T} \{\gamma^0\}^L + [HDH]^L \{K_\varepsilon\}^L = \sum_{I=1}^{N} [V]^{IL,T} \{v\}^{I,L} + \sum_{I \in \Lambda} [V_C]^{IL,T} \{b\}^{I,L}, L \in \lambda_C$		(VI.34-e)
$\sum_{J=1}^{N} B^{KJ} \{u\}^J + \sum_{J \in \Lambda}^{N} B_C^{KJ} \{a\}^J = \{\tilde{U}\}^K, \quad K = 1, M_u^O$	Compatibility equations with the imposed displacements on the edges of type O	(VI.35-a)
$\sum_{J=1}^{N} B^{KJ} \{u\}^J + \sum_{J \in \Lambda}^{N} B_C^{KJ} \{a\}^J = \{\tilde{U}\}^{A(K)}, \quad K = 1, M_u^A$	Compatibility equations with the imposed displacements on the edges of type H	(VI.35-b)
$\sum_{J=1}^{N} B^{KJ} \{u\}^J + \sum_{J \in \Lambda}^{N} B_C^{KJ} \{a\}^J = \{\tilde{U}\}^{B(K)}, \quad K = 1, M_u^B$		(VI.35-c)

$$\sum_{L=1}^{N}[M_{UU}]^{JL}\{u\}^{L}+\sum_{L\in\Lambda}[M_{UA}]^{JL}\{a\}^{L} -\left\{\sum_{K=1}^{M_u^O}B^{KJ}\{r\}^{K}+\sum_{K=1}^{M_u^A}B^{KJ}\{r\}^{A(K)}+\sum_{K=1}^{M_u^B}B^{KJ}\{r\}^{B(K)}\right\}=\{\widetilde{Q}\}^{J}$$ $$, \quad J=1,N$$	Equilibrium equation for each Voronoi cell	(VI.48)
$$\sum_{L=1}^{N}[M_{AU}]^{JL}\{u\}^{L}+\sum_{L\in\Lambda}[M_{AA}]^{JL}\{a\}^{L} -\left\{\sum_{K=1}^{M_u^O}B_C^{KJ}\{r\}^{K}+\sum_{K=1}^{M_u^A}B_C^{KJ}\{r\}^{A(K)}+\sum_{K=1}^{M_u^B}B_C^{KJ}\{r\}^{B(K)}\right\}=\{\widetilde{Q}_C\}^{J}$$ $$, \quad J\in\Lambda$$	Equilibrium equation for cells of type O and type H	(VI.56)

VI.5.4. Final equation system

Let:

$$\langle B_O\rangle=\langle B^{KJ}\rangle;\quad K=1,M_u^O;\ \langle B_A\rangle=\langle B^{KJ}\rangle;\quad K=1,M_u^A;\ \langle B_B\rangle=\langle B^{KJ}\rangle;\quad K=1,M_u^B$$

$$\langle B\rangle=\langle\langle B_O\rangle\ \ \langle B_A\rangle\ \ \langle B_B\rangle\rangle$$

$$\langle B_{CO}\rangle=\langle B_C^{KJ}\rangle;\quad K=1,M_u^O;\ \langle B_{CA}\rangle=\langle B_C^{KJ}\rangle;\quad K=1,M_u^A;\ \langle B_{CB}\rangle=\langle B_C^{KJ}\rangle;\quad K=1,M_u^B$$

$$\langle B_C\rangle=\langle\langle B_{CO}\rangle\ \ \langle B_{CA}\rangle\ \ \langle B_{CB}\rangle\rangle$$

$$[B_S]=\begin{bmatrix}\langle B\rangle\\ \langle B_C\rangle\end{bmatrix};\qquad \{r\}=\begin{Bmatrix}\{r\}^{K}\\ \{r\}^{A(K)}\\ \{r\}^{B(K)}\end{Bmatrix}$$

Then we have:

$$[B_S]\{r\}=\begin{Bmatrix}\left\{\sum_{K=1}^{M_u^O}B^{KJ}\{r\}^{K}+\sum_{K=1}^{M_u^A}B^{KJ}\{r\}^{A(K)}+\sum_{K=1}^{M_u^B}B^{KJ}\{r\}^{B(K)}\right\}\\ \left\{\sum_{K=1}^{M_u^O}B_C^{KJ}\{r\}^{K}+\sum_{K=1}^{M_u^A}B_C^{KJ}\{r\}^{A(K)}+\sum_{K=1}^{M_u^B}B_C^{KJ}\{r\}^{B(K)}\right\}\end{Bmatrix}$$

Combining equations (VI.48), (VI.56), (VI.35) gives an equation system of the form:

$$\begin{bmatrix}[KM] & -[B_S]\\ -[B_S]^T & [0]\end{bmatrix}\begin{Bmatrix}\{q\}\\ \{r\}\end{Bmatrix}=\begin{Bmatrix}\{\widetilde{Q}_S\}\\ -\{\widetilde{U}\}\end{Bmatrix}$$

with:

$$[KM]=\begin{bmatrix}[M_{UU}] & [M_{UA}]\\ [M_{AU}] & [M_{AA}]\end{bmatrix};\quad [B]=\begin{Bmatrix}[B]\\ [B_C]\end{Bmatrix};\ \{q\}=\begin{Bmatrix}\{u\}\\ \{a\}\end{Bmatrix};\quad \{\widetilde{Q}_S\}=\begin{Bmatrix}\{\widetilde{Q}\}\\ \{\widetilde{Q}_C\}\end{Bmatrix}$$

which is similar to the one obtained in linear elasticity (III.60).

It is easily proved that:

- $[M_{UU}]^{JL}=[M_{UU}]^{LJ,T},\quad J=1,N\quad L=1,N$
- $[M_{AA}]^{JL}=[M_{AA}]^{LJ,T},\quad J=1,N\quad L=1,N$
- $[M_{UA}]^{JL}=[M_{AU}]^{LJ,T},J=1,N\quad L\in\Lambda$

From the above equations, it is seen that the matrix $[KM]$ is symmetric.

Equations (VI.35) which, in matrix form, become $[B]^T\{q\}=\{\widetilde{U}\}$ constitute a set of constraints on the nodal displacements $\{q\}$. They can be used to remove some imposed displacements from the unknowns $\{q\}$as detailed in chapter III.

This leads to an equation system of the classical form $[M]\{q\}=\{\widetilde{Q}\}$.

After solving this system, the displacements are known and (VI.38) is used to compute the stress intensity coefficients $\{K_\Sigma\}^I$ at each crack tip.

VI.6. Applications

VI.6.1. Mode 1 tests

A simple tension case was performed for mode 1 as shown in figure VI.10.

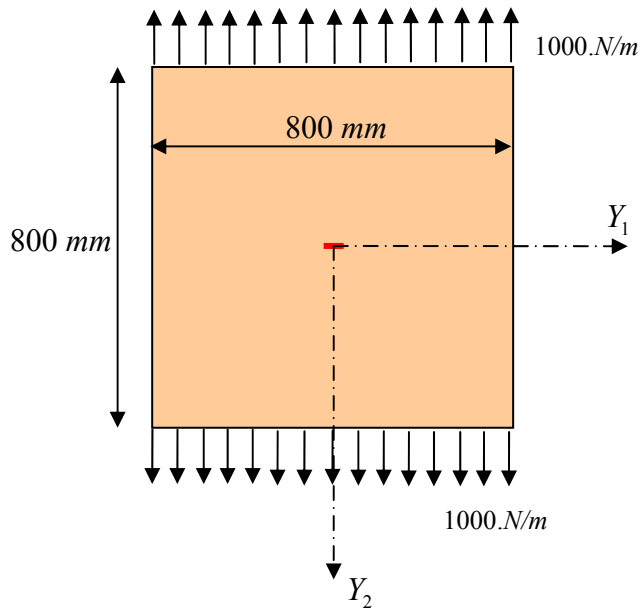

Figure VI.10. Mode 1 test loading in linear fracture mechanics.

In this case, plane stress state was assumed and the values of Young's modulus and Poisson's ratio were: $E = 200000\ MPa$ and $\nu = 0.3$.

The crack length is 120 mm.

A model with 387 nodes (361 regularly spaced nodes + 26 nodes near the crack tips) was generated as shown in figure VI.11.

Figure VI.12 shows a zoom near the crack tip.

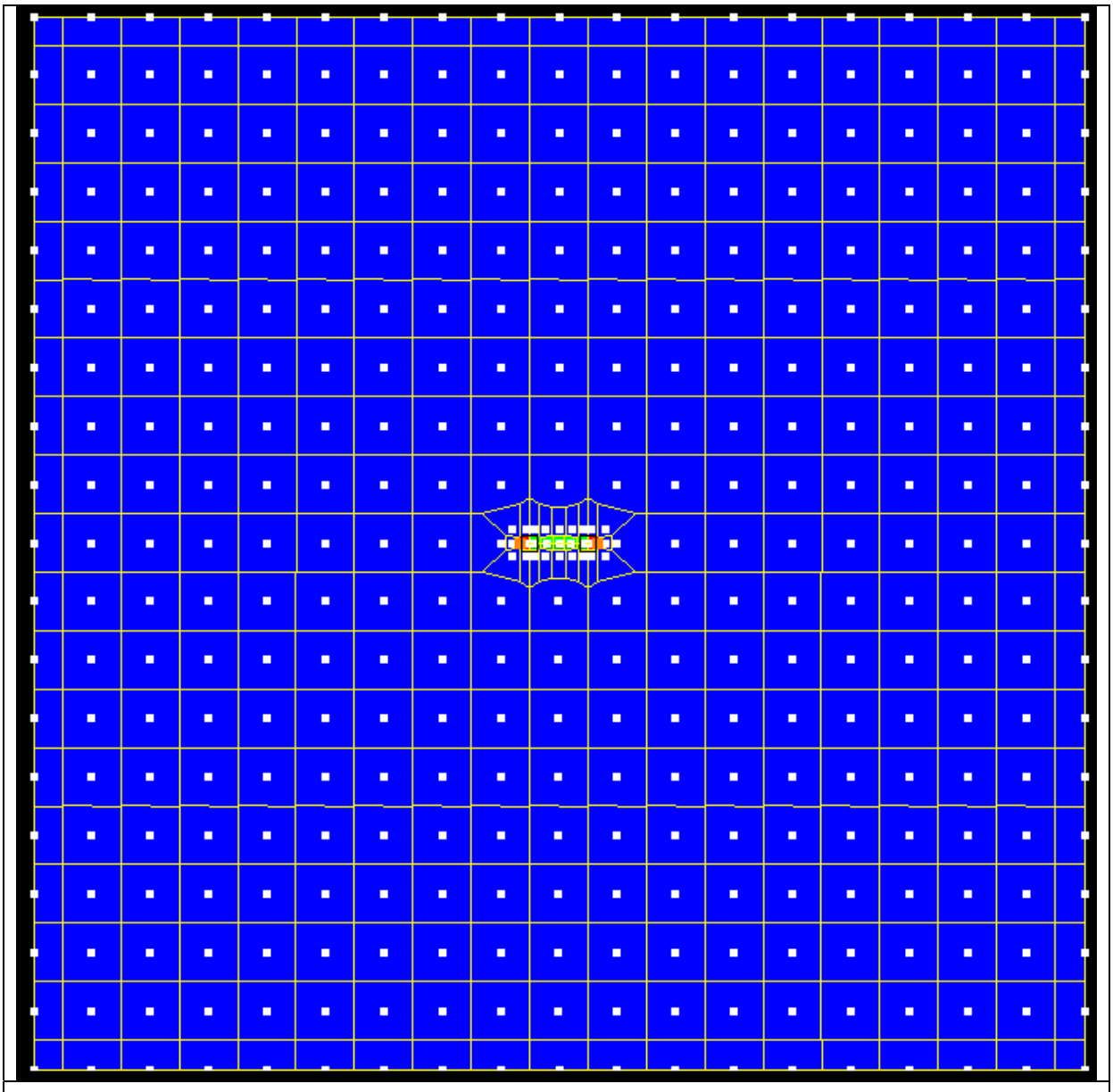

Figure VI.11. Short crack (120 mm) in tension : Voronoi cells 387 nodes

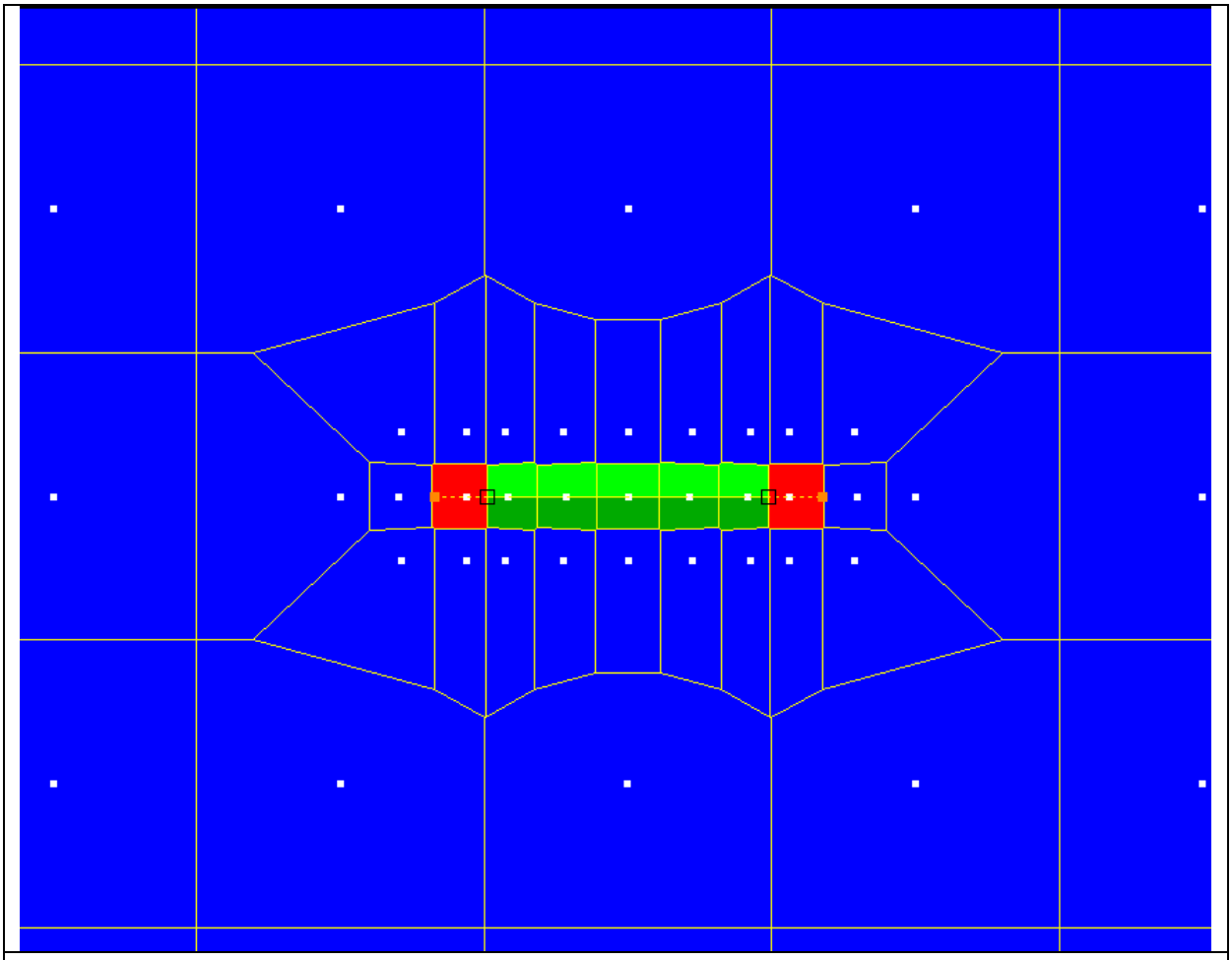

Figure VI.12. Short crack in tension : Voronoi cells with 387 nodes; zoom near the crack
Type C cells 2 parts of type H cells crack tips

The following notations were defined in sectionVI.3.4:

$\Lambda = \lambda^H \cup \lambda^C$

in which

λ^H is the set of nodes corresponding to all the cells of type H and λ^C is the set of nodes corresponding to all the cells of type C.

In this test, two different methods were used: method 0 and method 1.

- In Method 0, the set of displacement jump parameter a only takes account of λ^H.
- In Method 1, the set of displacement jump parameters a takes account of Λ, which is the union of λ^H and λ^C.

It is possible to use different numbers of integration points on cells of different types.

Figure VI.13 shows the evolution of $K_{\Sigma 1}$.

- Figure VI.13.a shows the results of $K_{\Sigma 1}$ for Method 0 and Method 1 with the same number of integration points used on all the cells.

- Figure VI.13.b only keeps the curve of Method 1 and adds another curve showing the results of Method 1 with different numbers of integration points used on cells of type C and cells of type H and O separately.

Figure VI.14 shows the evolution of the crack opening. The theoretical value is 1.20 mm.

- Figure VI.14.a shows the results of crack opening for Method 0 and Method 1 with the same number of integration points used on all the cells.
- Figure VI.14.b only keeps the curve of Method 1 and adds another curve showing the results of Method 1 with different numbers of integration points used on cells of type C and cells of type H and O separately.

In the new curves of figure VI.13.b and VI.14.b, 1000 integration points are used on the edges of cells of type C, other numbers of integration points are used on the edges of cells of type H and O.

For a number of integration points up to 32, Gauss integration scheme is used. For 1000 integration points, the trapeze integration scheme is used.

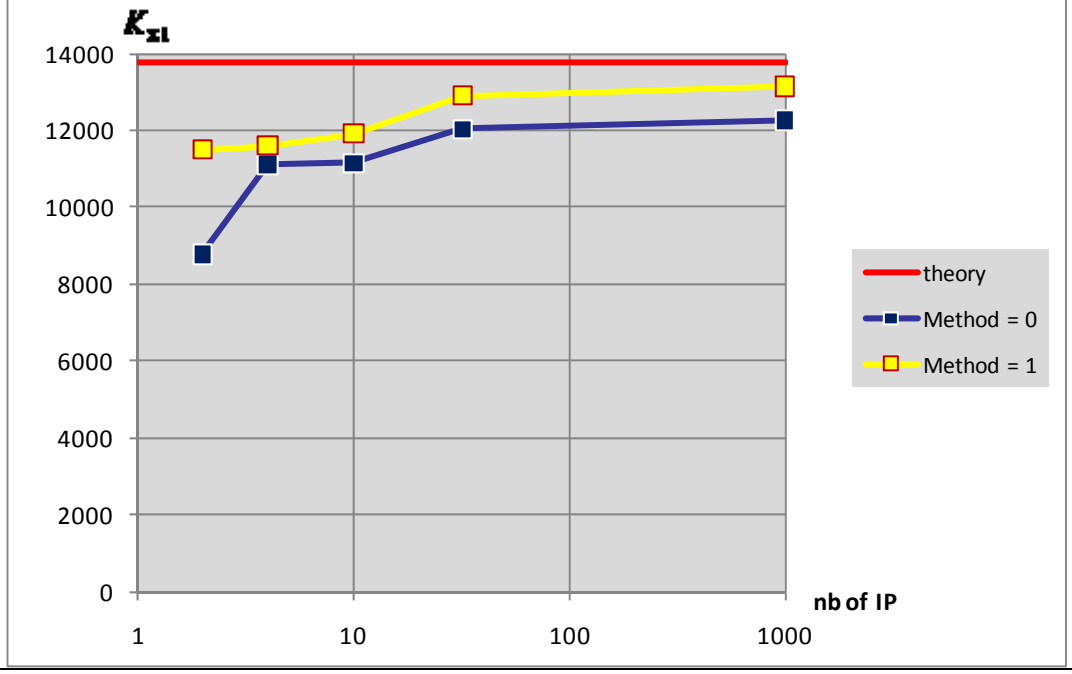

Figure VI.13.a. Evolution of $K_{\Sigma 1}$ for mode 1 with the same number of integration points on all the cells

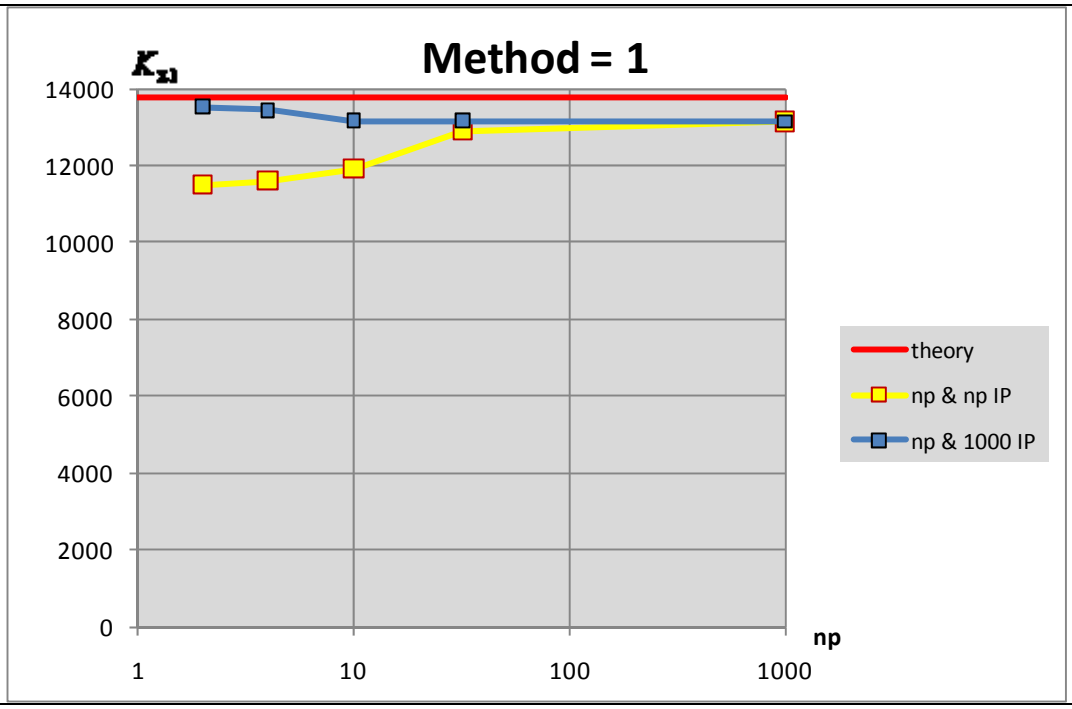

Figure VI.13.b. Evolution of $K_{\Sigma 1}$ for mode 1 with different numbers of integration points on cells of different types

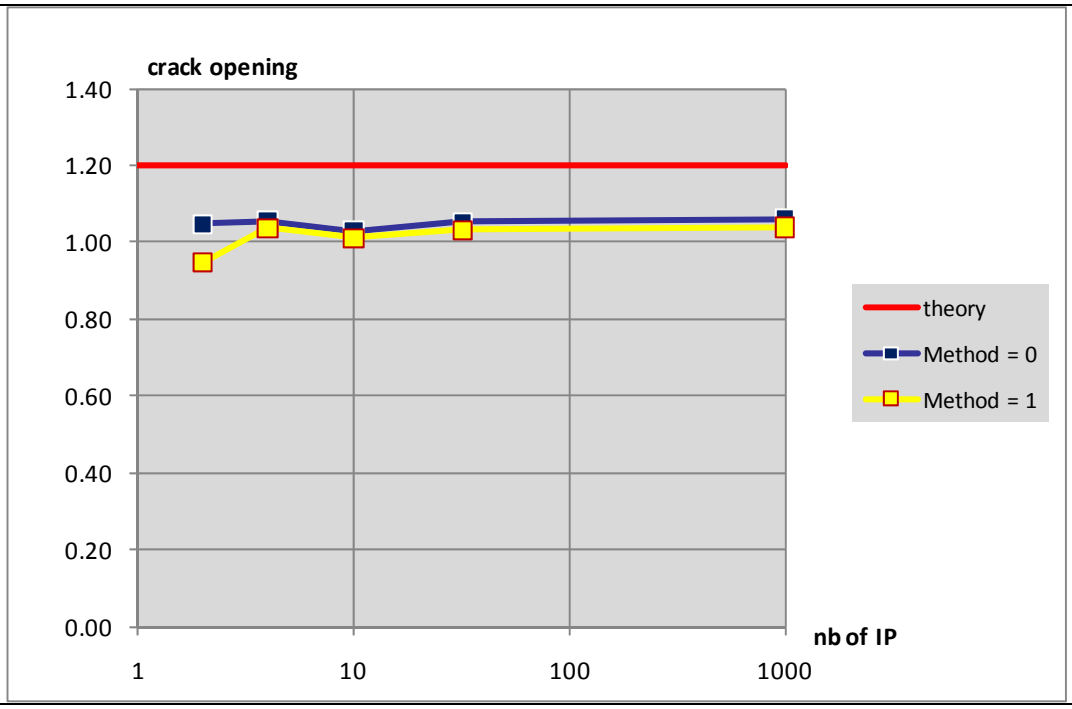

Figure VI.14.a. Evolution of the crack opening for mode 1 with the same number of integration points on all the cells

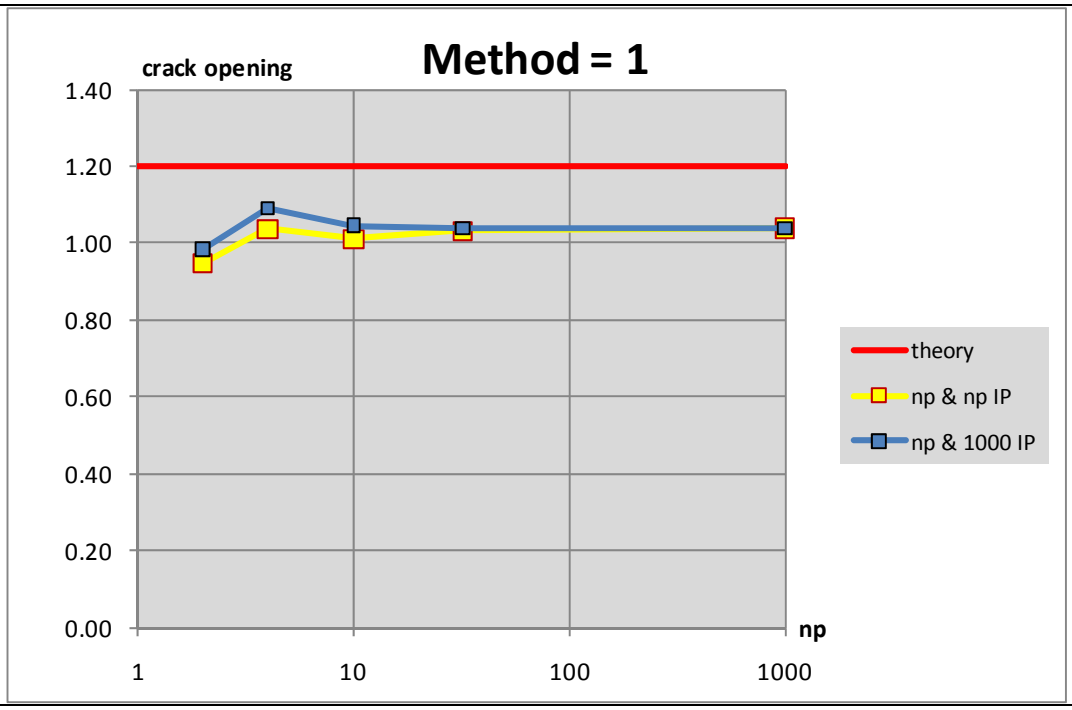

Figure VI.14.b. Evolution of a for mode 1 with different number of integration points on cells of different types

Figure VI.15 shows the crack opening (amplified by a factor 5).

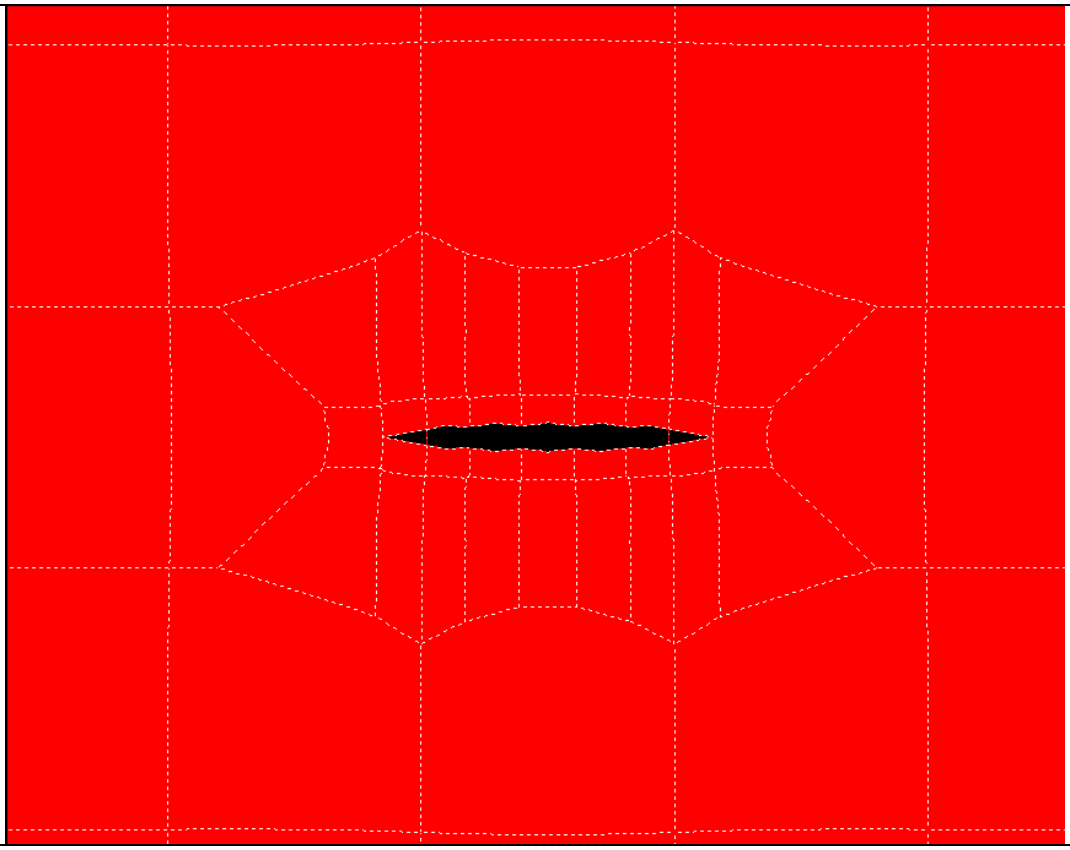

Figure VI.15. Short crack in tension : crack opening (amplified by a factor 5)

It must be noted that, to obtain good results, it is better to use 32 Gauss integration points on the edges of the crack tip cells (cells of type C). This can be attributed to the fact that the matrix $[V_C]$ (see table VI.6) computed by numerical integration on the edges of cells of type C, contains the functions $\{H_1\}$ and $\{H_2\}$ which are highly non linear.

Since the other matrices containing these functions (namely $[HDH]$ and $[IH]$) are computed analytically, $[V_C]$ must be obtained with sufficient precision. Indeed, all these matrices appear simultaneously in the equations (VI.38, 39) that allow calculating the stress intensity coefficients from the displacements $\{v\}$ and the displacement jumps $\{b\}$.

It is important to remark that nodes density near the crack tips is increased. This is necessary since there is only one cell (the cell of type C) to obtain the stress intensity coefficient at the crack tip. In that cell, the near crack tip approximations $\{H_1\}$ and $\{H_2\}$ are used so that this cell should have a small size with respect to the crack length. In the surrounding cells, the hypotheses of constant stresses and strains are used. Hence, to reasonably approximate the stress evolution in the vicinity of the crack tip, one should also have ordinary cells of small size.

An attempt to use large cells has been made but failed to produce acceptable results near the crack tip.

For this attempt, the regularly spaced 361 nodes of the preceding mesh were used without increasing the node density near the crack tips.

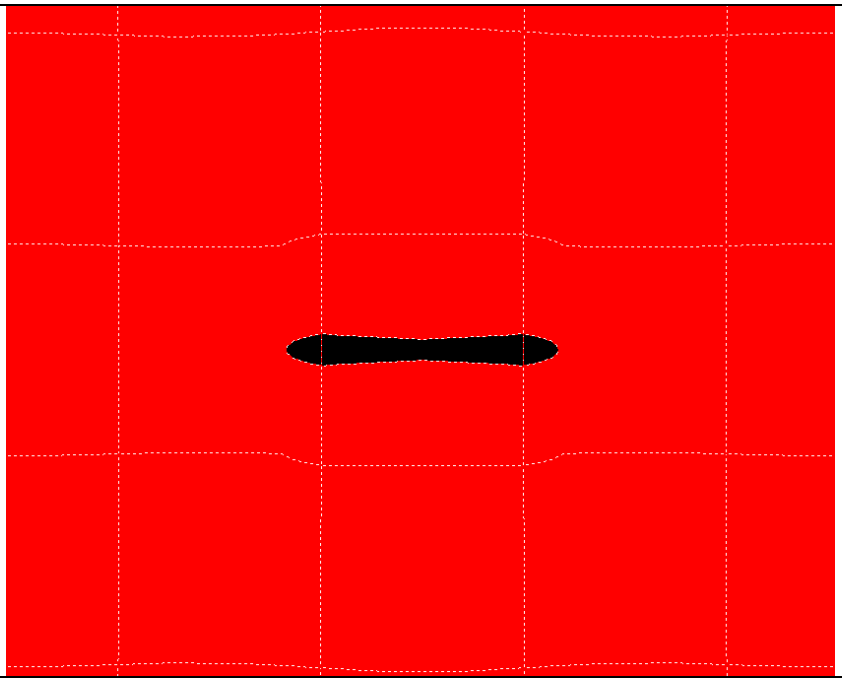

Figure VI.16. Short crack in tension: crack opening (amplified by a factor 5) with no increase of the node density near the crack tips; result for Method 1.

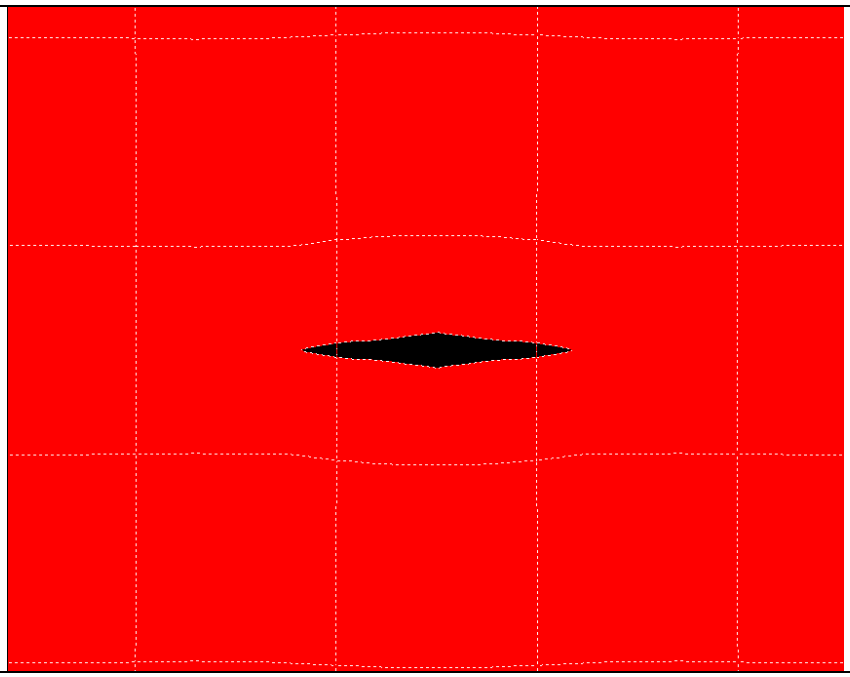

Figure VI.17. Short crack in tension: crack opening (amplified by a factor 5) with no increase of the node density near the crack tips; result for Method 0.

Figure VI.16 shows the shape of the crack obtained with Method 1 and 1000 integration points on the edges of the crack tip cells. The crack opening at the middle of the cell is 1.87 mm which is still acceptable considering the very rough approximation of the crack. However, the stress intensity coefficient is totally unrealistic: a negative value was obtained.

For the calculations with Method 0, all the other parameters remaining the same, the shape of the crack is given by figure VI.17. The crack opening at the middle of the cell is 1.61 mm and the value of the stress intensity coefficient is 4924. These results are clearly better than with Method 1 but, unsurprisingly, still far from the theoretical values.

VI.6.2. Mode 2 tests

With the same mesh (387 nodes, figures VI.11 and VI.12) as in mode 1 test, we can perform numerical tests for mode 2 as shown in figure VI.18.

The values of Young's modulus and Poisson's ratio are the same as for mode 1 test.

Plane stress state was also assumed and Method 1 was used.

Figure VI.19 shows the evolution of $K_{\Sigma 2}$ with different numbers of integration points on the edges of the Voronoi cells of type C.

Figure VI.20 shows the evolution of the displacement jump a_1 at the centre of the crack.

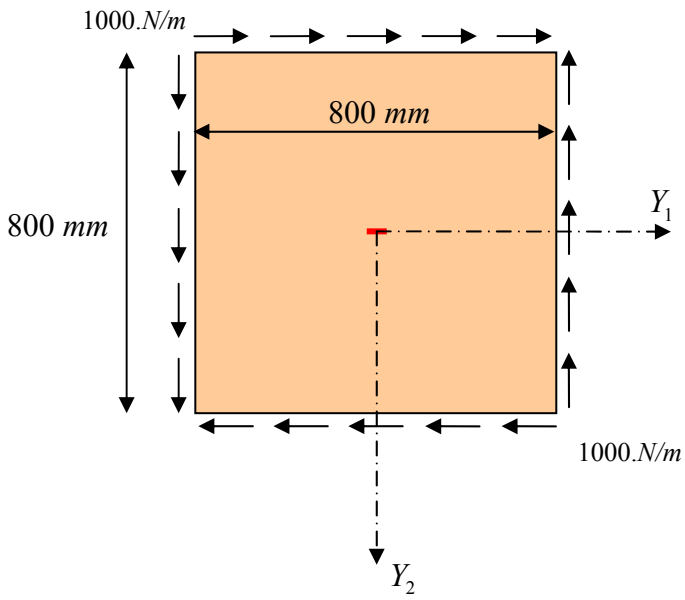

Figure V.18. Mode 2 test loading in linear elastic fracture mechanics

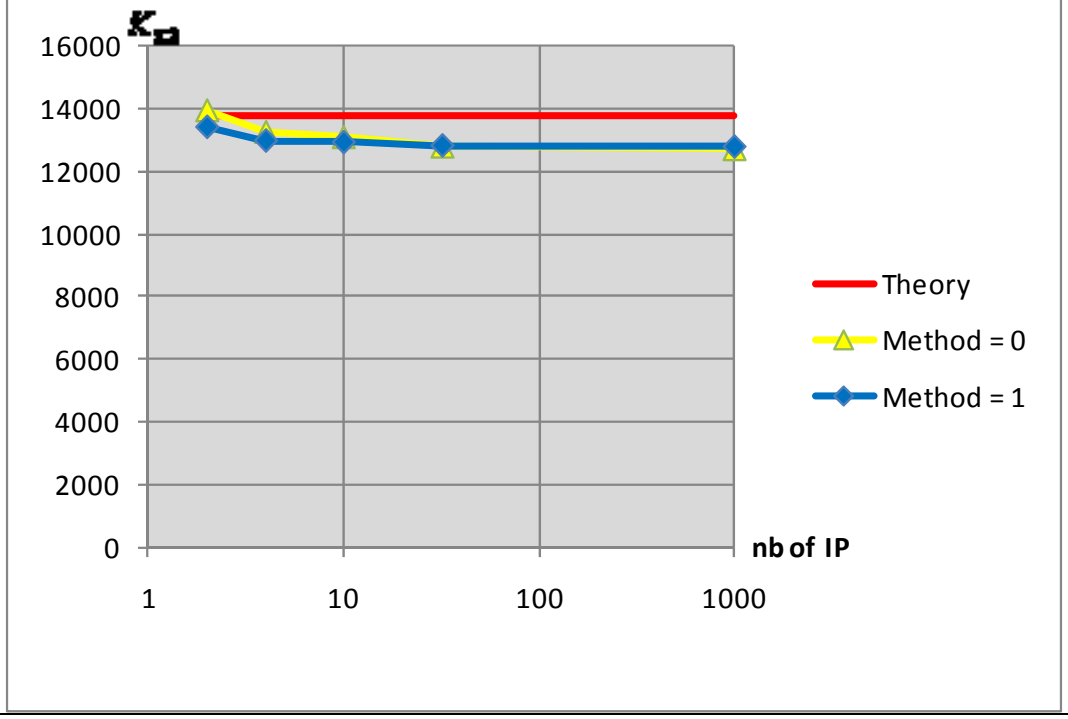

Figure VI.19. Evolution of $K_{\Sigma 2}$ for mode 2 with the number of integration points

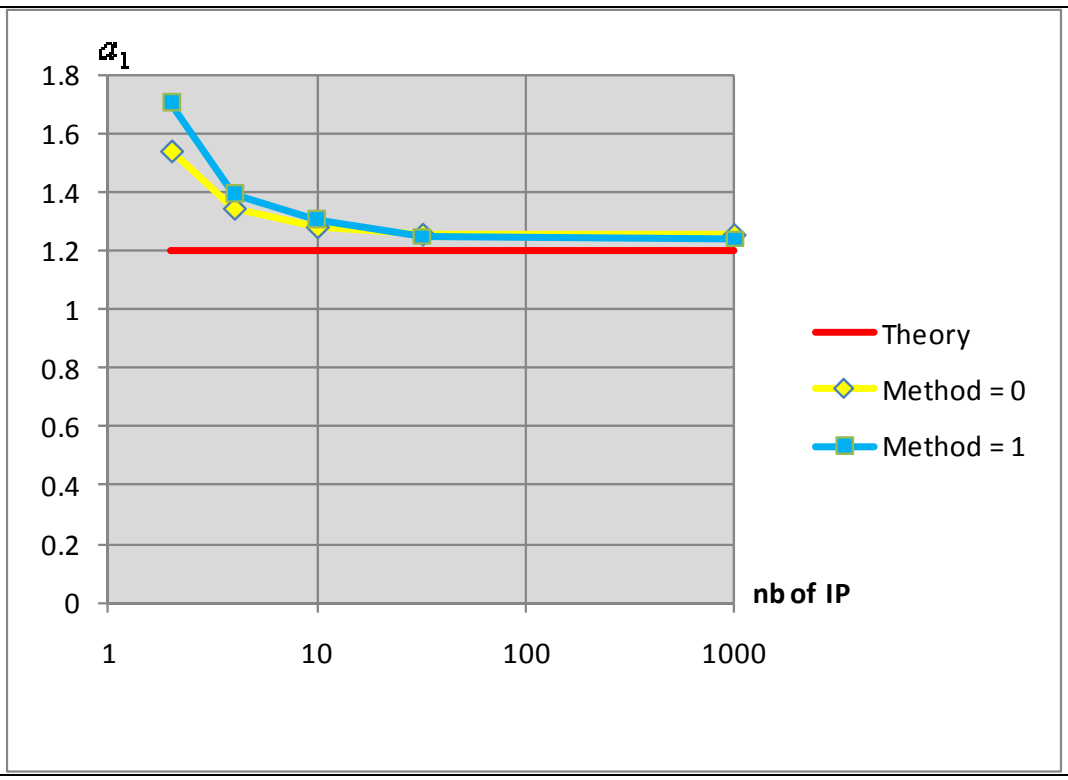

Figure VI.20. Evolution of a_1 with the number of integration points

The same remarks as for the mode 1 test apply.

VI.6.3 Single edge crack

A rectangular model was built for the single edge crack problem shown in figure VI.21.

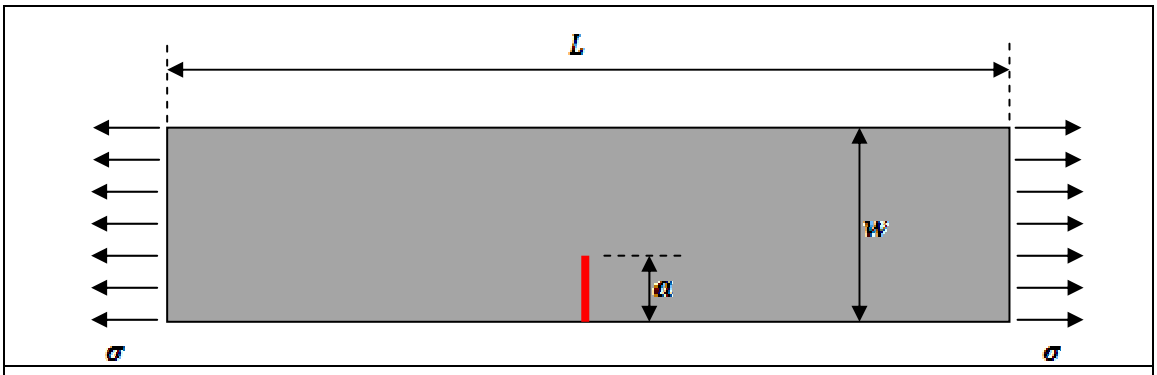

Figure VI.21. Bar with a single edge crack (not at scale)

The crack (in red) has no thickness and is located at mid span.

The values used for the computations are:

$L = 1600\ mm;\ w = 400 mm;\ a = 10\ mm, \sigma = 1000\ MPa$

$E = 200000\ MPa$ and $\nu = 0.3$

Plane stress state is considered.

The theoretical value of the stress intensity coefficient is given in [MIANNAY D. P. (1998)] for $L \to \infty$:

$$K_I = \sigma\sqrt{w}\,\frac{\sqrt{2\tan\frac{\pi a}{w}}}{\cos\frac{\pi a}{w}}\left[0.752 + 2.02\,\frac{a}{w} + 0.37\,\left(1 - \sin\frac{\pi a}{w}\right)^3\right] \qquad \text{(VI.58)}$$

The computations were performed for different numbers of nodes and different numbers of integration points

Only Method 1 was applied in this case.

Three different meshes were tested.

Figure VI.22 shows the Voronoi cells for mesh n° 1 (322 nodes) and figure VI.23 shows a zoom near the crack.

Figure VI.24 shows the Voronoi cells for mesh n° 2 (612 nodes) and figure VI.25 shows a zoom near the crack.

Figure VI.26 shows the Voronoi cells for mesh n° 3 (612 nodes) and figure VI.27 shows a zoom near the crack.

In mesh n° 2, the Voronoi cells corresponding to the contour nodes near the crack tip are large. This may have an influence on the results. Mesh n° 3 is obtained from mesh n° 2 by moving the contour nodes closer to the crack tip. With these two different meshes, we can see the dependency of the results on the mesh near the crack tip.

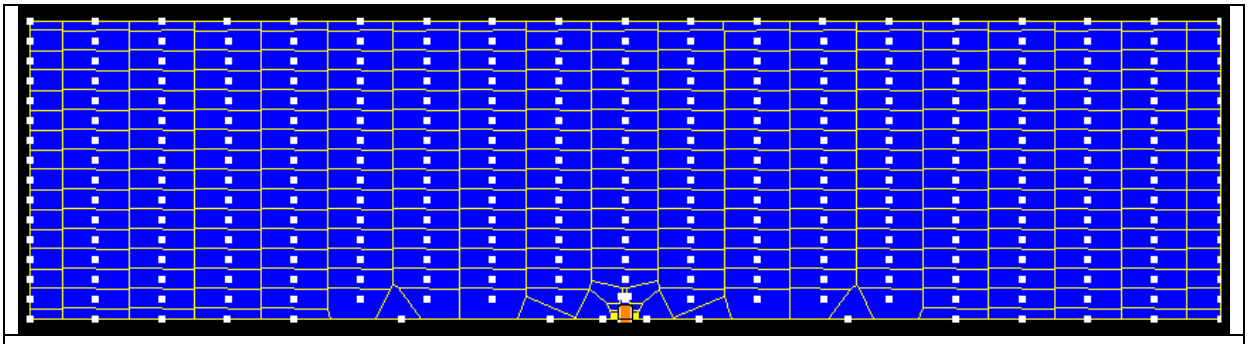

Figure VI.22. Single edge crack : mesh n° 1 (322 nodes) ; whole structure

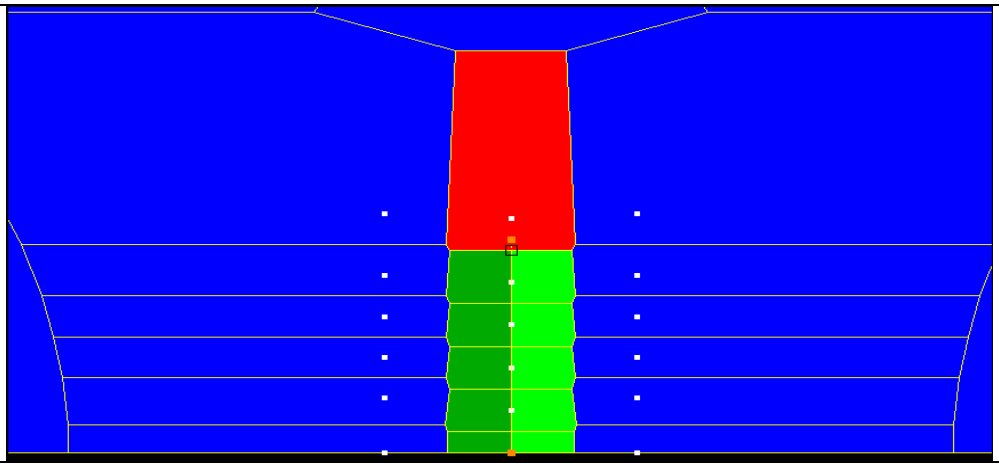

Figure VI.23. Single edge crack : mesh n° 1 (322 nodes) ; zoom near the crack

Type C cell 2 parts of type H cells crack tip

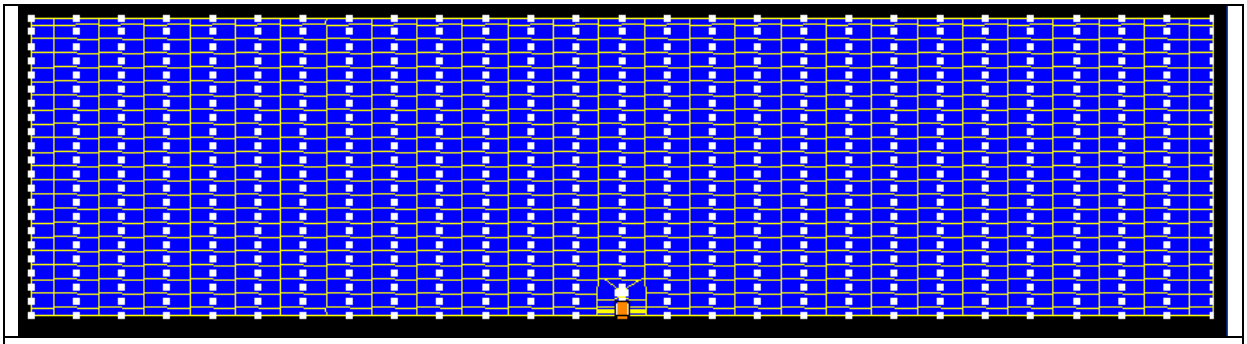

Figure VI.24. Single edge crack : mesh n° 2 (612 nodes) ; whole structure

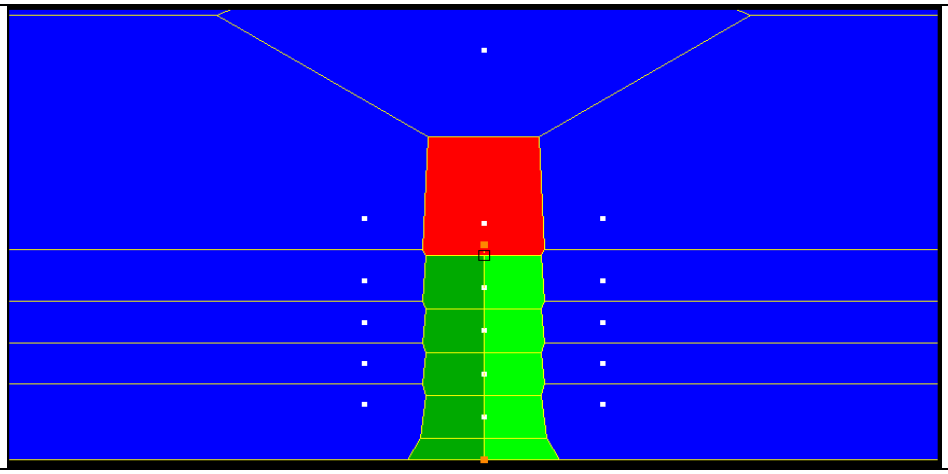

Figure VI.25. Single edge crack : mesh n° 2 (612 nodes) ; zoom near the crack

Type C cell 2 parts of type H cells crack tip

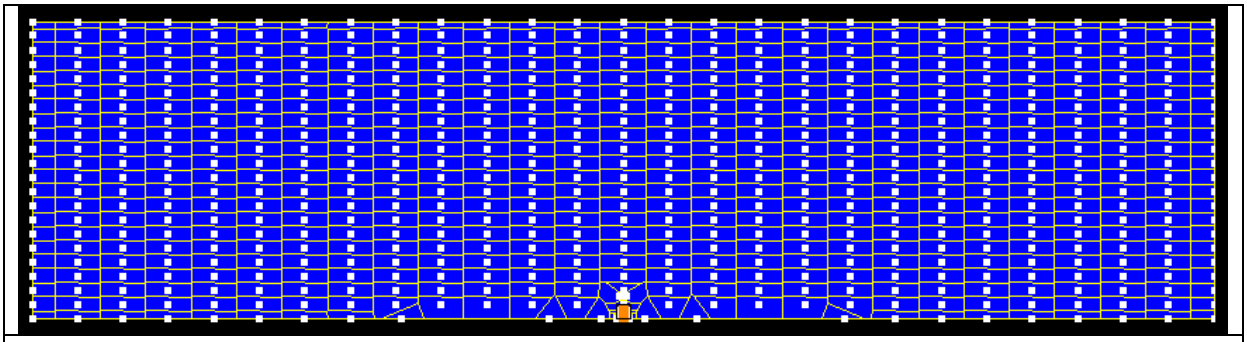

Figure VI.26. Single edge crack : mesh n° 3 (612 nodes) ; whole structure

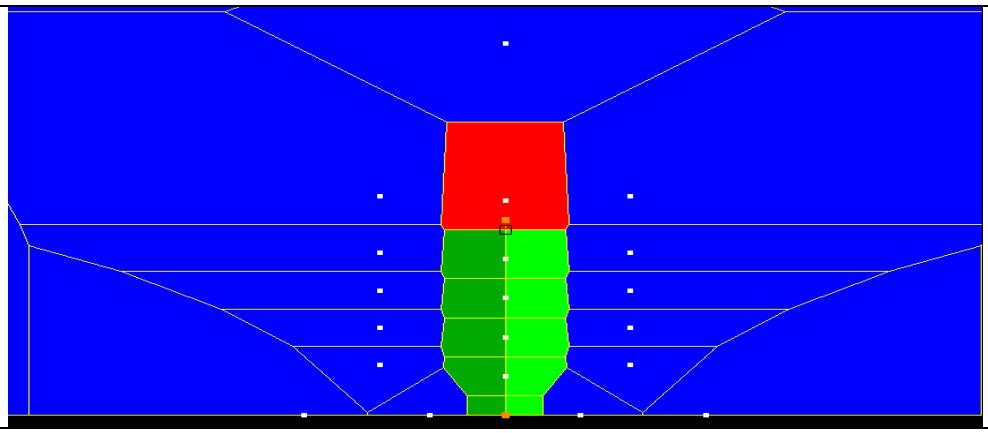

Figure VI.27. Single edge crack : mesh n° 3 (612 nodes) ; zoom near the crack

Type C cell 2 parts of type H cells crack tip

Figure VI.28 and VI.29 show the evolution of $K_{\Sigma 1}$ and of the crack opening with the number of integration points. We can see that the quality of the Voronoi cells around the crack plays an important role. Large cells decrease the quality of the results.

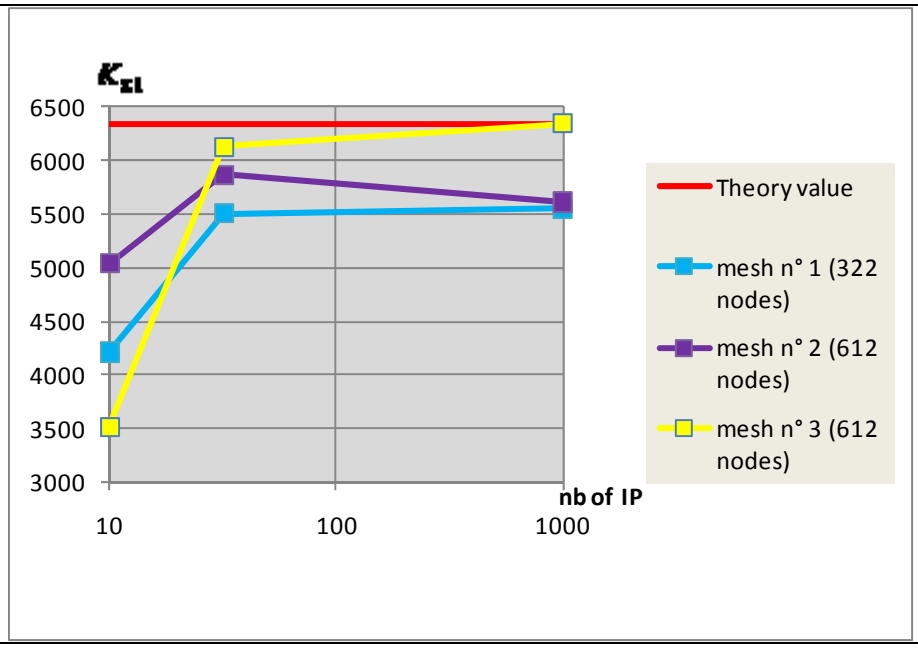

Figure VI.28. Evolution of $K_{\Sigma 1}$ for the single edge crack problem

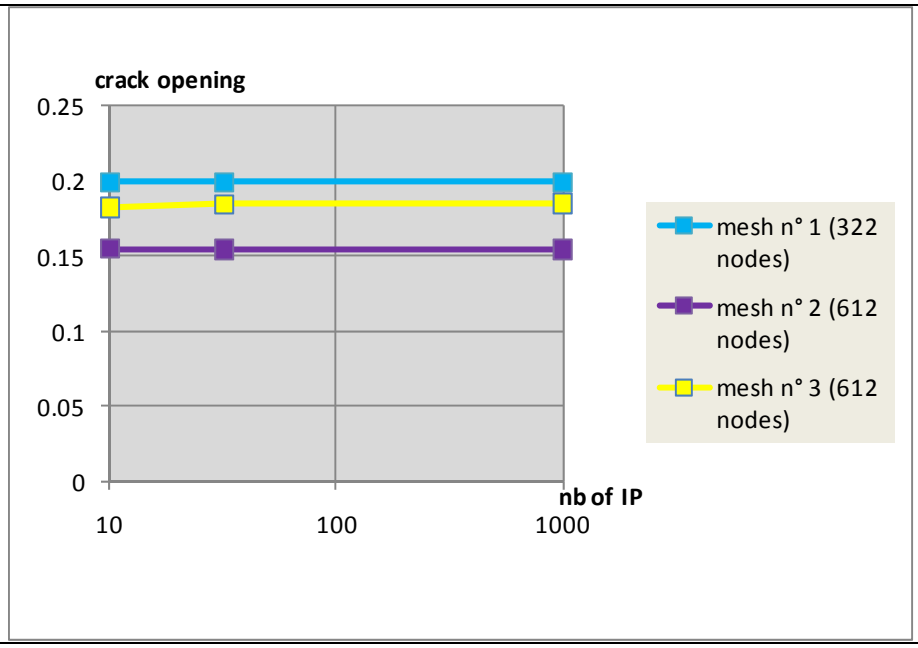

Figure VI.29. Evolution of the crack opening for the single edge crack problem

VI.6.4 Nearly incompressible case

In order to check that incompressibility locking is avoided in the present case, the calculations have been performed for the single edge crack problem (figure VI.21) with a Poisson's ratio close to 0.5.

The results are collected in figure VI.30.

It is seen that there is no incompressible locking.

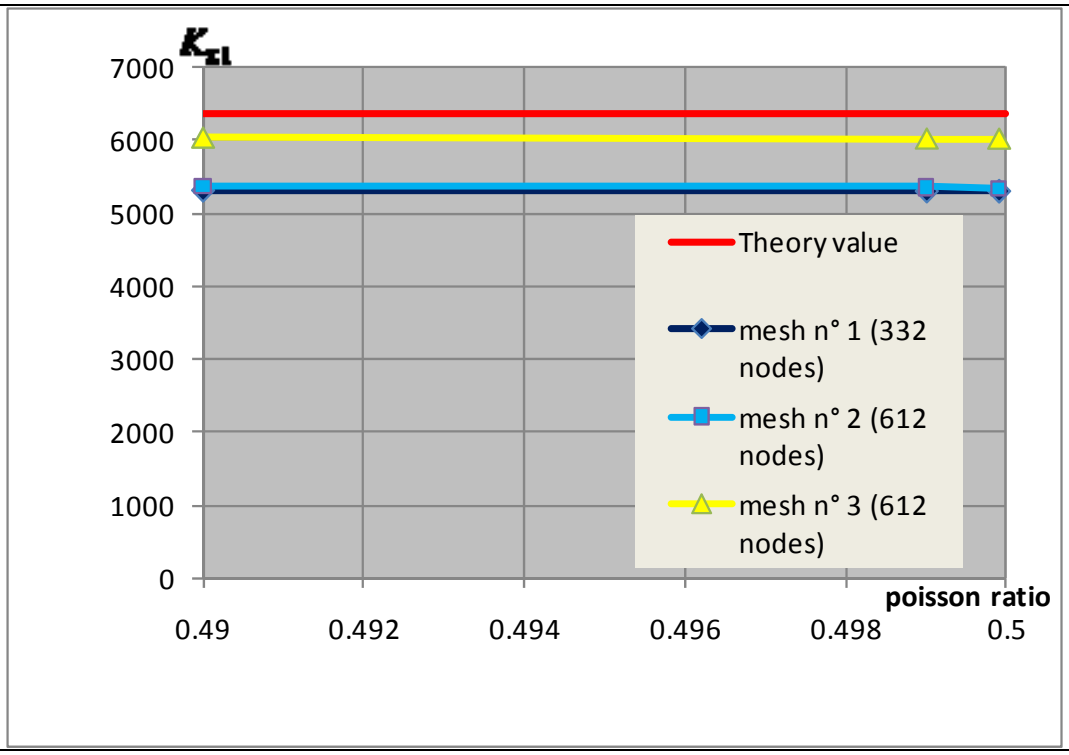

Figure VI.30. Single edge crack test for a nearly incompressible material with 1000 integration points

VI.7. Conclusion

The Fraeijs de Veubeke variational principle has been used to develop a constraint natural neighbours method in which the displacements, stresses, strains and surface support reactions can be discretized separately.

By introducing a line to present the crack that does not confirm to the nodes or the edges of the Voronoi cells, an eXtended Natural nEighbour Method (XNEM) is developed to solve 2D problems of LEFM.

We have 3 types of cells:

- cells of type *O* that do not contain a crack;
- cells of type *H* that are divided into 2 parts by a crack;
- cells of type *C* that contain a crack tip.

An assumption on the stresses deduced from the exact solution of Westergaard [WESTERGAARD, H.M. (1939)] has been introduced in the cells of type C by which the stress intensity coefficients become primary variables of the method.

The assumed stresses, strains and support reactions are constant over the cells of type O and over each part of the cells of type H.

Introducing all the assumptions and enrichments in the FdV variational principle produces the set of equations governing the discretized solid.

The additional degrees of freedom linked with the assumed stresses and strains can be eliminated at the level of the Voronoi cells, finally leading to a system of equations of the same type as in the classical displacement-based method: 2 classical degrees of freedom are associated with each node but there is a set of additional parameters: displacement jump parameters that describe the discontinuity through the crack.

In cells of type C, some integrals over the area remain but they can be calculated analytically so that, in the formulation, only numerical integrations on the edges of the cells of type C are required.

In cells of type O and H, the calculations of integrals over the area is avoided: only integrations on the edges of the Voronoi cells are required.

In all the cases, the derivatives of the nodal shape functions are not required in the resulting formulation.

As in chapters III, IV and V, the displacements can be imposed in 2 ways:

- In the spirit of the FdV variational principle, boundary conditions of the type $u_i = \widetilde{u}_i$ on S_u can be imposed in the average sense; hence, any function $\widetilde{u}_i = \widetilde{u}_i(s)$ can be accommodated by the method;
- However, since the natural neighbours method is used, the interpolation of displacements on the solid boundary is linear between 2 adjacent nodes. So, if the imposed displacements $\widetilde{u}_i$ are linear between 2 adjacent nodes, they can be imposed exactly. This is obviously the case with $\widetilde{u}_i = 0$. In such a case, it is equivalent to impose the displacements of these 2 adjacent nodes to zero.

Applications to the mode 1 test, mode 2 test and single edge crack test are performed.

Two different methods are examined in mode 1 test: Method 0 and Method 1

- In Method 0, no displacement jump parameters are associated with the cells of type C
- In Method 1, the displacement jump parameters take account of the union of type C cells and type H cells

It is observed that these two methods don't give significantly different results.

Different meshes are generated to evaluate the dependency of the results on the meshes.

The results of mode 1 test and single edge crack test show that the node density near the crack tip plays a central role. In cells of type C, the near crack tip approximations $\{H_1\}$ and $\{H_2\}$ are used so that this cell should have a small size with respect to the crack length. In the surrounding cells, the hypotheses of constant stresses and strains are used. Hence, to reasonably approximate the stress evolution in the vicinity of the crack tip, one should also have ordinary cells of small size.

It is also worth mentioning that using 32 integration points of the Gauss integration scheme or 1000 integration points of the trapeze integration scheme on the edges of type C cells makes the results much better.

Running the single edge test with a Poisson's ratio close to 0.5 proves that the nearly incompressibility locking is avoided.